either condition (Fig. 5*Bii*), and CMA did not affect the cytotoxic activities against Jurkat cells, irrespective of the culture conditions (data not shown). This finding suggests that perforin or granzyme B does not have a major role in killing Jurkat cells. We evaluated whether TRAIL had a role by adding anti-TRAIL-blocking Ab RIK2 to the medium. RIK2 partially but clearly suppressed the cytotoxic activities against Jurkat cells generated in both conditions without significant differences (Fig. 5*Bii*), although TRAIL expression was slightly higher in the NK cells generated in the D4-Fc plus IL-15 condition (Fig. 5*Cii*). From these observations, we concluded that IL-15 does not influence the killing activity through TRAIL but does enhance the killing activity through perforin/granzyme B. The cytotoxic activity of immature NK cells is TRAIL dependent, while that of mature NK cells is mainly dependent on perforin (29). Therefore, IL-15 might contribute to the maturation of NK cells and confer on them the capacity to exact perforin/granzyme B-medicated cytotoxicity.

Inhibitory effect of anti-Notch1 Ab on Delta4-dependent NK cell development

We prepared mAbs specific for the extracellular domain of Notch1, Notch2, and Notch3 (supplemental Fig. S4*A*). The expression patterns of Notch1, Notch2, and Notch3 in fresh CB mononuclear cells, $CD34^+$ cells, and products during the culture of $CD34^+$ cells are shown in supplemental Fig. S3, *A* and *B*. Notch1 was expressed at higher levels on NK and T cells than on B cells and monocytes. Notch2 was expressed at higher levels on monocytes than on lymphocytes. Notch3 expression was virtually negative on all types of lymphocytes and positive on monocytes. Notch1 and Notch2, but not Notch3, were expressed on $CD34^+$ cells. The $CD34^+$ cell-derived $CD56^+$ NK cells also expressed Notch1 and Notch2, but not Notch3. All three Notch receptors were expressed on cells grown on the control Fc-coated plates (supplemental Fig. S3*B*).

Because $CD34^+$ cells expressed Notch1 and Notch2, but not Notch3 (supplemental Fig. S3*B*), and the established anti-Notch1 Ab, but not anti-Notch2 Ab, blocked binding of the cognate soluble Notch receptor to the ligands (supplemental Fig. S4*B*), we cultured CB $CD34^+$ cells on Delta4-Fc-coated plates in anti-Notch1 Ab-containing medium. Remarkably, the immunophenotype of the cells grown under the presence of anti-Notch1 Ab was almost the same as that of cells grown on control Fc-coated plates, indicating that the effect of Delta4 was completely blocked and NK cell development was shut down by the anti-Notch1 Ab (Fig. 6*A*). Anti-Notch2 Ab did not have such an effect, consistent with the fact that it did not block ligand binding to the cognate receptors (data not shown). CB $CD34^+$ cells cultured with IL-15 on Fc-coated plates in the presence of the anti-Notch1 Ab gave rise to NK cells in a manner indistinguishable from that of cells grown without the Ab (Fig. 6*B*). These results suggest that Notch1 might be a physiologic Notch receptor that mediates Delta4 signaling for NK cell development from CB $CD34^+$ cells and further support the notion that Notch signaling has a role distinct from that of IL-15.

Discussion

In the present study, we demonstrated that functional NK cells developed from CB $CD34^+$ cells when stimulated with the Notch ligand Delta4. Previous reports indicated that NK cells can be derived from in vitro culture of human $CD34^+$ cells prepared from fetal liver, bone marrow, or CB with either IL-2 or IL-15 (30–33), which signal through the shared IL-2/IL-15 receptor β-chain and the common γ-chain. IL-15 has been considered to have a more physiologic role than IL-2 in NK development (30). Notably, IL-15-independent NK cell differentiation has recently been published (6). This culture system, however, has been reported to be stromal cell dependent while the potential molecules and signaling pathways are unknown and, thus, the conclusion whether IL-15 is indispensable is yet to be determined. Notch signaling has been examined in the context of NK cell development as well and appears to affect the very early phase of progenitor development (17–19). In studies of human NK cell development, however, culture systems containing IL-15 and/or a coculture system with the fetal thymus organ or stromal cells are used exclusively. A novel and unexpected finding in the present study was the fact that stimulation of CB $CD34^+$ cells with a soluble Notch ligand, Delta4-Fc, coated onto the plate in the presence of stem cell factor, FL, and IL-7 was sufficient to induce the development of functional NK cells.

Our data do not officially exclude the possibility that endogenous IL-15 is involved in NK cell development in a manner, e.g., that cell-autonomously produced IL-15 activated the signaling by binding to the receptor intracellularly. Given the fact, however, that the exogenous addition of IL-15 resulted in the qualitative rather than quantitative difference in the NK cells developed in the presence of Delta4-Fc, in addition to inefficient blockade by anti-IL-15-neutralizing Ab, IL-15 is likely to be dispensable for human NK cell development in the presence of Delta4-Fc.

The finding that IL-15 is not necessary for human NK cell development in culture contrasts with the absolute necessity of IL-15 signaling for NK development in some mouse phenotypes; mice lacking a gene for IL-15 (3) (34, 35), IL-15 receptor α-chain (36), common β-chain (37), or common γ-chain (38, 39) lack NK cells. This might be due to differences between the in vitro culture conditions and the in vivo environment in which NK cells develop. Another explanation might be a difference between mice and humans, as in the case of IL-7 requirement for T cell development; IL-7 is required for the V-D-J rearrangement of the TCR β-chain gene in humans, whereas it is dispensable in mouse T cell development (40).

Previous studies reported that the effect of Notch signaling in the presence of IL-15 on NK cell development is confined to the very early stages of development. In the present study, we demonstrated that Notch signaling confers CD7 expression competence on cells cultured with or without IL-15 for 1 wk or less, but not for 2 wk, unless also stimulated by Notch. This finding is similar to that in a previous report demonstrating that Notch signaling confers cyCD3 expression competence only on prethymic but not thymic NK cell progenitors or peripheral blood $cyCD3^-$ NK cells (19). We confirmed the Notch signal dependency of cyCD3 expression during NK cell development. Coexpression of CD7 and CD45RA on $CD34^+$ cells might be associated with a restriction toward NK cell development (26, 33). Our data strongly suggest that the vast majority, if not all, of the NK cells derived from $CD34^+$ cells without Notch signaling were generated through $CD7^-$ cells. Therefore, although it is yet to be elucidated whether all of the NK cell progenitors are $CD7^+$ (41), NK cells established in vitro without Notch stimulation might not develop from a physiologic NK progenitor or might skip the physiologic NK/T progenitor stage. Furthermore, our data suggest that the effect of Notch stimulation on CD7 expression is imprinted on cells only if it is administered at the initial stage of the $CD34^+$ cell culture. We, however, failed to prospectively identify the subpopulations in the $CD34^+$ cells that are targets of Delta4 to develop NK-lineage cells. Delta4 stimulation induced NK cell development from both the most immature $CD34^+CD38^-$ and more mature $CD34^+CD38^+$ progenitor populations and both $CD34^+$

$CD45RA^+$ lymphoid progenitors and $CD34^+CD45RA^-$ populations (data not shown).

The findings of the present study extend our understanding to more mature stages of NK cell differentiation: the presence of Notch signaling induces generation of functional NK cells in culture conditions that do not generate $CD56^+$ cells without Notch stimulation per se. The precise stages of NK cell development during which Notch signaling determines the progression toward functional NK cells is not known.

In our experiments, even cells cultured with a Notch ligand alone had cytotoxic activity. The level of this activity, however, was weaker than that in NK cells generated by Notch stimulation with IL-15. Indeed, the perforin-mediated cytotoxicity of NK cells generated in the absence of IL-15 was significantly weaker, despite the fact that this is the major pathway of mature NK cells to kill target cells (42). In contrast, the TRAIL-mediated cytotoxicity was almost the same regardless of presence or absence of IL-15. This finding, along with the change in the expression level of CD56, might indicate that IL-15 induces the maturation of $CD56^{low}$ $CD161^+$ immature NK cells generated by Notch stimulation without IL-15. Another difference between the cells cultured with or without IL-15 was the down-regulation of adhesion molecules (CD11a, CD11b, CD62L) on the cell surface. These molecules might be important for homing of the NK cells to the sites at which they function.

To our surprise, cytotoxic activities were not detected in the cell populations generated in the control Fc plus IL-15 condition at either 3 or 6 wk (Fig. 5*B* and data not shown), although these results might be affected by the facts that the frequency of $CD56^+CD161^+$ cells was very low at 3 wk and that culture for 6 wk might be too long to evaluate cytotoxic activities while the frequency of $CD56^+CD161^+$ cells was much greater. In any case, when clinical application of progenitor-derived NK cells is considered, a Delta4-Fc-coating system would give a significant advantage.

In conclusion, Notch stimulation by Delta4 (or Delta1) was required for initial NK cell differentiation and the development of $CD161^+CD56^{low}$ immature NK cells. Among Notch receptors, Notch1 might be essential for physiologic NK cell development, although the involvement of other Notch receptors is yet to be elucidated. IL-15 was not essential for differentiation, but was necessary for maturation. IL-15 might have an indispensable role only in the later part of the NK development. This knowledge might be useful for future approaches toward the ex vivo generation and manipulation of NK cells and their therapeutic application.

Acknowledgments

We thank Y. Mori and E. Nakasone for providing excellent technical assistance.

Disclosures

The authors have no financial conflict of interest.

References

1. Freud, A. G., and M. A. Caligiuri. 2006. Human natural killer cell development. *Immunol. Rev.* 214: 56–72.
2. Hayakawa, Y., N. D. Huntington, S. L. Nutt, and M. J. Smyth. 2006. Functional subsets of mouse natural killer cells. *Immunol. Rev.* 214: 47–55.
3. Kennedy, M. K., M. Glaccum, S. N. Brown, E. A. Butz, J. L. Viney, M. Embers, N. Matsuki, K. Charrier, L. Sedger, C. R. Willis, et al. 2000. Reversible defects in natural killer and memory CD8 T cell lineages in interleukin 15-deficient mice. *J. Exp. Med.* 191: 771–780.
4. Williams, N. S., J. Klem, I. J. Puzanov, P. V. Sivakumar, J. D. Schatzle, M. Bennett, and V. Kumar. 1998. Natural killer cell differentiation: insights from knockout and transgenic mouse models and in vitro systems. *Immunol. Rev.* 165: 47–61.
5. Yokoyama, W. M., S. Kim, and A. R. French. 2004. The dynamic life of natural killer cells. *Annu. Rev. Immunol.* 22: 405–429.
6. McCullar, V., R. Oostendorp, A. Panoskaltsis-Mortari, G. Yun, C. T. Lutz, J. E. Wagner, and J. S. Miller. 2008. Mouse fetal and embryonic liver cells differentiate human umbilical cord blood progenitors into CD56-negative natural killer cell precursors in the absence of interleukin-15. *Exp. Hematol.* 36: 598–608.
7. Chiba, S. 2006. Concise review: Notch signaling in stem cell systems. *Stem Cells* 24: 2437–2447.
8. Artavanis-Tsakonas, S., M. D. Rand, and R. J. Lake. 1999. Notch signaling: cell fate control and signal integration in development. *Science* 284: 770–776.
9. Suzuki, T., and S. Chiba. 2005. Notch signaling in hematopoietic stem cells. *Int. J. Hematol.* 82: 285–294.
10. Radtke, F., A. Wilson, G. Stark, M. Bauer, J. v. Meerwijk, H. R. MacDonald, and M. Aguet. 1999. Deficient T cell fate specification in mice with an induced inactivation of Notch1. *Immunity* 10: 547–558.
11. Wilson, A., H. R. MacDonald, and F. Radtke. 2001. Notch 1-deficient common lymphoid precursors adopt a B cell fate in the thymus. *J. Exp. Med.* 194: 1003–1012.
12. Pui, J. C., D. Allman, L. Xu, S. DeRocco, F. G. Karnell, S. Bakkour, J. Y. Lee, T. Kadesch, R. R. Hardy, J. C. Aster, and W. S. Pear. 1999. Notch1 expression in early lymphopoiesis influences B versus T lineage determination. *Immunity* 11: 299–308.
13. Jaleco, A. C., H. Neves, E. Hooijberg, P. Gameiro, N. Clode, M. Haury, D. Henrique, and L. Parreira. 2001. Differential effects of Notch ligands Delta-1 and Jagged-1 in human lymphoid differentiation. *J. Exp. Med.* 194: 991–1002.
14. De Smedt, M., I. Hoebeke, K. Reynvoet, G. Leclercq, and J. Plum. 2005. Different thresholds of Notch signaling bias human precursor cells toward B-, NK-, monocytic/dendritic-, or T-cell lineage in thymus microenvironment. *Blood* 106: 3498–3506.
15. van den Brandt, J., K. Voss, M. Schott, T. Hunig, M. S. Wolfe, and H. M. Reichardt. 2004. Inhibition of Notch signaling biases rat thymocyte development towards the NK cell lineage. *Eur. J. Immunol.* 34: 1405–1413.
16. Garcia-Peydro, M., V. G. de Yebenes, and M. L. Toribio. 2006. Notch1 and IL-7 receptor interplay maintains proliferation of human thymic progenitors while suppressing non-T cell fates. *J. Immunol.* 177: 3711–3720.
17. Rolink, A. G., G. Balciunaite, C. Demoliere, and R. Ceredig. 2006. The potential involvement of Notch signaling in NK cell development. *Immunol. Lett.* 107: 50–57.
18. Carotta, S., J. Brady, L. Wu, and S. L. Nutt. 2006. Transient Notch signaling induces NK cell potential in Pax5-deficient pro-B cells. *Eur. J. Immunol.* 36: 3294–3304.
19. De Smedt, M., T. Taghon, I. Van de Walle, G. De Smet, G. Leclercq, and J. Plum. 2007. Notch signaling induces cytoplasmic CD3ε expression in human differentiating NK cells. *Blood* 110: 2696–2703.
20. Karanu, F. N., B. Murdoch, T. Miyabayashi, M. Ohno, M. Koremoto, L. Gallacher, D. Wu, A. Itoh, S. Sakano, and M. Bhatia. 2001. Human homologues of Delta-1 and Delta-4 function as mitogenic regulators of primitive human hematopoietic cells. *Blood* 97: 1960–1967.
21. Kayagaki, N., N. Yamaguchi, M. Nakayama, A. Kawasaki, H. Akiba, K. Okumura, and H. Yagita. 1999. Involvement of TNF-related apoptosis-inducing ligand in human $CD4^+$ T cell-mediated cytotoxicity. *J. Immunol.* 162: 2639–2647.
22. Kataoka, T., N. Shinohara, H. Takayama, K. Takaku, S. Kondo, S. Yonehara, and K. Nagai. 1996. Concanamycin A, a powerful tool for characterization and estimation of contribution of perforin- and Fas-based lytic pathways in cell-mediated cytotoxicity. *J. Immunol.* 156: 3678–3686.
23. Shimizu, K., S. Chiba, K. Kumano, N. Hosoya, T. Takahashi, Y. Kanda, Y. Hamada, Y. Yazaki, and H. Hirai. 1999. Mouse Jagged1 physically interacts with Notch2 and other Notch receptors. *J. Biol. Chem.* 274: 32961–32969.
24. Geling, A., H. Steiner, M. Willem, L. Bally-Cuif, and C. Haass. 2002. A γ-secretase inhibitor blocks Notch signaling in vivo and causes a severe neurogenic phenotype in zebra fish. *EMBO Rep.* 3: 688–694.
25. Cheng, H.-T., J. H. Miner, M. Lin, M. G. Tansey, K. Roth, and R. Kopan. 2003. γ-Secretase activity is dispensable for mesenchyme-to-epithelium transition but required for podocyte and proximal tubule formation in developing mouse kidney. *Development* 130: 5031–5042.
26. Haddad, R., P. Guardiola, B. Izac, C. Thibault, J. Radich, A.-L. Delezoide, C. Baillou, F. M. Lemoine, J. C. Gluckman, F. Pflumio, and B. Canque. 2004. Molecular characterization of early human T/NK and B-lymphoid progenitor cells in umbilical cord blood. *Blood* 104: 3918–3926.
27. Sanchez, M., M. Muench, M. Roncarolo, L. Lanier, and J. Phillips. 1994. Identification of a common T/natural killer cell progenitor in human fetal thymus. *J. Exp. Med.* 180: 569–576.
28. Huntington, N. D., C. A. J. Vosshenrich, and J. P. Di Santo. 2007. Developmental pathways that generate natural-killer-cell diversity in mice and humans. *Nat. Rev. Immunol.* 7: 703–714.
29. Zamai, L., M. Ahmad, I. M. Bennett, L. Azzoni, E. S. Alnemri, and B. Perussia. 1998. Natural killer (NK) cell-mediated cytotoxicity: differential use of TRAIL and Fas ligand by immature and mature primary human NK cells. *J. Exp. Med.* 188: 2375–2380.
30. Mrozek, E., P. Anderson, and M. Caligiuri. 1996. Role of interleukin-15 in the development of human $CD56^+$ natural killer cells from $CD34^+$ hematopoietic progenitor cells. *Blood* 87: 2632–2640.
31. Jaleco, A., B. Blom, P. Res, K. Weijer, L. Lanier, J. Phillips, and H. Spits. 1997. Fetal liver contains committed NK progenitors, but is not a site for development of $CD34^+$ cells into T cells. *J. Immunol.* 159: 694–702.

32. Lotzova, E., C. Savary, and R. Champlin. 1993. Genesis of human oncolytic natural killer cells from primitive $CD34^+CD33^-$ bone marrow progenitors. *J. Immunol.* 150: 5263–5269.
33. Miller, J., K. Alley, and P. McGlave. 1994. Differentiation of natural killer (NK) cells from human primitive marrow progenitors in a stroma-based long-term culture system: identification of a $CD34^+7^+$ NK progenitor. *Blood* 83: 2594–2601.
34. Ohteki, T., H. Yoshida, T. Matsuyama, G. S. Duncan, T. W. Mak, and P. S. Ohashi. 1998. The transcription factor interferon regulatory factor 1(IRF-1) is important during the maturation of natural killer 1.1^+ T cell receptor-α/β^+ ($NK1^+$ T) cells, natural killer cells, and intestinal intraepithelial T cells. *J. Exp. Med.* 187: 967–972.
35. Ogasawara, K., S. Hida, N. Azimi, Y. Tagaya, T. Sato, T. Yokochi-Fukuda, T. A. Waldmann, T. Taniguchi, and S. Taki. 1998. Requirement for IRF-1 in the microenvironment supporting development of natural killer cells. *Nature* 391: 700–703.
36. Lodolce, J. P., D. L. Boone, S. Chai, R. E. Swain, T. Dassopoulos, S. Trettin, and A. Ma. 1998. IL-15 receptor maintains lymphoid homeostasis by supporting lymphocyte homing and proliferation. *Immunity* 9: 669–676.
37. Suzuki, H., G. S. Duncan, H. Takimoto, and T. W. Mak. 1997. Abnormal development of intestinal intraepithelial lymphocytes and peripheral natural killer cells in mice lacking the IL-2 receptor β chain. *J. Exp. Med.* 185: 499–506.
38. Cao, X., E. W. Shores, J. Hu-Li, M. R. Anver, B. L. Kelsall, S. M. Russell, J. Drago, M. Noguchi, A. Grinberg, E. T. Bloom, et al. 1995. Defective lymphoid development in mice lacking expression of the common cytokine receptor γ chain. *Immunity* 2: 223–238.
39. DiSanto, J., W. Muller, D. Guy-Grand, A. Fischer, and K. Rajewsky. 1995. Lymphoid development in mice with a targeted deletion of the interleukin 2 receptor γ chain. *Proc. Natl. Acad. Sci. USA* 92: 377–381.
40. Spits, H. 2002. Development of $\alpha\beta$ T cells in the human thymus. *Nat. Rev. Immunol.* 2: 760–772.
41. Freud, A. G., A. Yokohama, B. Becknell, M. T. Lee, H. C. Mao, A. K. Ferketich, and M. A. Caligiuri. 2006. Evidence for discrete stages of human natural killer cell differentiation in vivo. *J. Exp. Med.* 203: 1033–1043.
42. Smyth, M. J., E. Cretney, J. M. Kelly, J. A. Westwood, S. E. A. Street, H. Yagita, K. Takeda, S. L. H. van Dommelen, M. A. Degli-Esposti, and Y. Hayakawa. 2005. Activation of NK cell cytotoxicity. *Mol. Immunol.* 42: 501–510.

Derivation of functional mature neutrophils from human embryonic stem cells

Yasuhisa Yokoyama,[1-3] Takahiro Suzuki,[1,2,4] Mamiko Sakata-Yanagimoto,[1-3] Keiki Kumano,[1,2] Katsumi Higashi,[5] Tsuyoshi Takato,[4] Mineo Kurokawa,[2] Seishi Ogawa,[1,4,6] and Shigeru Chiba[1,3]

[1]Department of Cell Therapy and Transplantation Medicine, University of Tokyo Hospital, Tokyo; [2]Department of Hematology and Oncology, Graduate School of Medicine, University of Tokyo, Tokyo; [3]Department of Clinical and Experimental Hematology, University of Tsukuba, Ibaraki; [4]Divison of Tissue Engineering, University of Tokyo Hospital, Tokyo; [5]Department of Clinical Hematology, School of Health Sciences, Kyorin University, Tokyo; and [6]The 21st Century COE Program, Graduate School of Medicine, University of Tokyo, Tokyo, Japan

Human embryonic stem cells (hESCs) proliferate infinitely and are pluripotent. Only a few reports, however, describe specific and efficient methods to induce hESCs to differentiate into mature blood cells. It is important to determine whether and how these cells, once generated, behave similarly with their in vivo–produced counterparts. We developed a method to induce hESCs to differentiate into mature neutrophils. Embryoid bodies were formed with bone morphogenic protein-4, stem cell factor (SCF), Flt-3 ligand (FL), interleukin-6 (IL-6)/IL-6 receptor fusion protein (FP6), and thrombopoietin (TPO). Cells derived from the embryoid bodies were cultured on a layer of irradiated OP9 cells with a combination of SCF, FL, FP6, IL-3, and TPO, which was later changed to granulocyte–colony-stimulating factor. Morphologically mature neutrophils were obtained in approximately 2 weeks with a purity and efficiency sufficient for functional analyses. The population of predominantly mature neutrophils (hESC-Neu's) showed superoxide production, phagocytosis, bactericidal activity, and chemotaxis similar to peripheral blood neutrophils from healthy subjects, although there were differences in the surface antigen expression patterns, such as decreased CD16 expression and aberrant CD64 and CD14 expression in hESC-Neu's. Thus, this is the first description of a detailed functional analysis of mature hESC-derived neutrophils. (Blood. 2009;113:6584-6592)

Introduction

Embryonic stem (ES) cells can self-renew and differentiate into cells derived from all 3 germ layers (ie, ectoderm, endoderm, and mesoderm). Both mouse and human ES cells give rise to mature blood cells of granulocyte/macrophage, erythroid, and megakaryoid lineages in vitro. For blood cell induction from ES cells, the majority of investigators use a coculturing system with mouse stromal cells such as S17[1] or OP9.[2,3] Embryoid body (EB) formation is also a commonly used method to obtain starting materials for further culture.[4-6] Cell surface antigens, such as CD45 and CD34, and colony-forming ability are used as blood cell markers. Hemangioblasts, which have the capacity to differentiate into both endothelial and blood cells, have also been produced.[7-9] Only a few studies, however, have achieved specific and effective induction of mature blood cells from ES cells, particularly human ES cells (hESCs).[10]

Human ESC-derived blood cells are potentially useful as a replacement for donation-based blood for transfusion in clinical settings, for drug discovery screening, and for monitoring drug efficacy and toxicity. The current blood donation system for transfusion is incapable of providing enough granulocytes for patients with life-threatening neutropenia, although granulocyte transfusion could have a potentially significant benefit for a certain population of severely neutropenic patients.[11,12] Given the large amount of neutrophils required for transfusion,[13] hESC-derived neutrophils might be a unique solution for this treatment demand. Therefore, the development of a highly effective method of neutrophil differentiation from hESCs is an important step for both clinical application of hESCs and granulocyte transfusion medicine.

The lack of an effective method for obtaining hESC-derived neutrophils with purity sufficient for functional analysis, however, has hampered progress in this field. Once neutrophils with a high purity can be generated from hESCs, it will be important to compare their activities with those of neutrophils produced in vivo, particularly given the fact that hESCs rarely give rise to hematopoietic stem cells in vitro,[14] and thus, that hESC-derived neutrophils might not be a progeny of hematopoietic stem cells. Here, we developed an effective method of deriving mature neutrophils from hESCs through EB formation and subsequent coculture with OP9, and analyzed their morphologic and phenotypic characteristics. We then performed functional analyses of hESC-derived neutrophils in vitro, focusing on superoxide production, phagocytosis, bactericidal activity, and chemotaxis, in comparison with peripheral blood neutrophils (PB-Neu's) obtained from healthy subjects.

Methods

Human ES cell culture and EB formation

In all experiments using hESCs, we used KhES-3[15] cells (a kind gift from Dr Nakatsuji; Kyoto University, Kyoto, Japan), which were maintained as previously described.[16] Briefly, KhES-3 colonies were cultured on irradiated mouse embryonic fibroblasts in Dulbecco modified Eagle medium/F12 (Invitrogen, Carlsbad, CA) supplemented with 20% KNOCKOUT serum

Submitted May 31, 2008; accepted March 5, 2009. Prepublished online as *Blood* First Edition paper, March 25, 2009; DOI 10.1182/blood-2008-06-160838.

An Inside *Blood* analysis of this article appears at the front of this issue.

The publication costs of this article were defrayed in part by page charge payment. Therefore, and solely to indicate this fact, this article is hereby marked "advertisement" in accordance with 18 USC section 1734.

replacer (Invitrogen) and 2.5 ng/mL human basic fibroblast growth factor (Invitrogen). The culture medium was replaced daily with fresh medium. Colonies were passaged onto new mouse embryonic fibroblasts every 6 days. To induce the formation of EBs, KhES-3 colonies were picked up using collagenase, and cultured in suspension in nonserum stem cell medium that we previously used in a hematopoietic stem cell expansion protocol.[17] After 24 hours, the colonies formed EBs, which were collected and cultured further for 17 days in Iscove modified Dulbecco medium (IMDM; Invitrogen) containing 15% fetal bovine serum (FBS), 1% nonessential amino acid (Invitrogen), 2 mM L-glutamine, 100 U/mL penicillin, 100 μg/mL streptomycin, and 0.1 mM 2-mercaptoethanol (ME) supplemented with cytokines (25 ng/mL bone morphogenic protein-4 [R&D Systems, Minneapolis, MN], 50 ng/mL stem cell factor [SCF; R&D Systems], 50 ng/mL Flt-3 ligand [R&D Systems], 50 ng/mL interleukin-6 [IL-6]/IL-6 receptor fusion protein [FP6; Kyowa Hakko Kirin, Tokyo, Japan], and 20 ng/mL thrombopoietin [TPO; Kyowa Hakko Kirin]).

Expansion of hematopoietic progenitor cells and terminal differentiation into mature neutrophils on OP9 stromal cells

OP9 cells (a kind gift from Dr Nakano; Osaka University, Osaka, Japan) were irradiated with 20 Gy and plated onto gelatin-coated 6-well tissue culture plates at a density of 1.5×10^5/well. The next day, the EBs (incubated for 18 days after the initiation of suspension culture) were trypsinized and disrupted into single cells. Cells were suspended in the progenitor expansion medium (IMDM supplemented with 10% FBS, 10% horse serum [StemCell Technologies, Vancouver, BC], 5% protein-free hybridoma medium [Invitrogen], 0.1 mM 2-ME, 100 U/mL penicillin, 100 μg/mL streptomycin, 100 ng/mL SCF, Flt-3 ligand, FP6, and 10 ng/mL TPO and IL-3 [R&D Systems]) and plated onto the irradiated OP9 cells (day 0). Each well contained up to 5×10^5 EB-derived cells. The culture medium was replaced with fresh medium on day 4.

On day 7 of the progenitor expansion phase, floating cells were collected, suspended with terminal differentiation medium (IMDM supplemented with 10% FBS, 0.1 mM 2-ME, 100 U/mL penicillin, 100 μg/mL streptomycin, and 50 ng/mL granulocyte colony-stimulating factor [G-CSF; Kyowa Hakko Kirin]), and transferred onto the newly irradiated OP9 cells. The culture medium was replaced with fresh medium on day 10. This terminal differentiation phase culture was continued for 6 or 7 days.

Preparation of normal PB-Neu's and bone marrow mononuclear cells

Human peripheral blood and bone marrow cells were obtained from healthy adult donors after obtaining informed consent in accordance with the Declaration of Helsinki. The institutional review board of the University of Tsukuba approved the use of peripheral blood neutrophils in this research. PB-Neu's were prepared as previously described.[18] The purity of the neutrophils was greater than 90%, with the remaining cells mainly eosinophils. Neutrophils were suspended in Hanks balanced salt solution (HBSS; Invitrogen) containing 0.5% bovine serum albumin (BSA) and placed at 4°C. In some experiments, peripheral blood mononuclear cells (PB-MNCs) were collected from the intermediate layer after centrifugation with Lymphoprep (Axis-shield, Oslo, Norway). Bone marrow cells were directly centrifuged with Lymphoprep, and only mononuclear cells were collected. Bone marrow mononuclear cells (BM-MNCs) were used immediately for RNA extraction.

Wright-Giemsa, myeloperoxidase, and alkaline-phosphatase staining

The morphology and granule characteristics of hESC-derived cells at the indicated days were assessed by Wright-Giemsa staining, comparing them with normal PB-Neu's. Myeloperoxidase and alkaline-phosphatase staining was performed using the New PO-K staining kit and alkaline phosphatase staining kit (MUTO PURE CHEMICALS, Tokyo, Japan). The prepared slides were inspected using an Olympus BX51 microscope equipped with a 100 × /1.30 UPlan objective lens (Olympus, Tokyo, Japan). Images were acquired with an HC-2500 digital camera and Photograb-2500 software (Fujifilm, Tokyo, Japan).

Electron microscopy

After 13 or 14 days culture, the population contained predominantly morphologically mature neutrophils, and was defined as hESC-Neu's. The hESC-Neu's and PB-Neu's were fixed in 2% paraformaldehyde/2.5% glutaraldehyde in 0.1 M phosphate buffered saline (PBS; Invitrogen) for at least 12 hours, and then postfixed in 1% osmium tetroxide in 0.1 M PBS for 2 hours. After fixation, samples were dehydrated in a graded ethanol series, cleared with propylene oxide, and embedded in Epon. Thin sections of cured samples were stained with uranyl acetate and Reynolds lead citrate. The sections were inspected using a transmission electron microscope, H7000 (Hitachi, Tokyo, Japan).

Semiquantitative RT-PCR for lactoferrin

Total RNA was obtained from hESC-derived cells of indicated culture days, PB-Neu's, PB-MNC's, and BM-MNC's using an RNeasy mini kit (QIAGEN, Hilden, Germany), and cDNA was synthesized from each RNA sample using a random primer and SuperScript III (Invitrogen) following the manufacturer's protocol. Semiquantitative polymerase chain reaction (PCR) was performed as previously described.[19] The sequence information of gene-specific primers used in reverse transcription (RT)–PCR and the PCR conditions is available upon request.

Flow cytometric analysis

Surface antigens of hESC-derived cells harvested on the indicated days were analyzed by flow cytometry using fluorescence-activated cell sorting (FACS) Aria (Becton Dickinson Immunocytometry Systems, San Jose, CA). Fc receptors on the cells were blocked with PBS containing 2% FBS and FcR Blocking Reagent (Miltenyi Biotec, Bergisch Gladbach, Germany). Antigens were stained with either fluorescein isothiocyanate (FITC)–conjugated antihuman CD13, CD64, CD11b (Beckman Coulter, Fullerton, CA), or CD14 (BD Pharmingen, San Diego, CA) antibodies; phycoerythrin-conjugated antihuman CD16, CD32, CD33 (Beckman Coulter), CD11b, or CD45 (BD Pharmingen) antibodies; or allophycocyanin-conjugated antihuman CD15, CD117 (BD Pharmingen), CD34, or CD133 (Myltenyi Biotec) antibodies. The negative range was determined by referencing the fluorescence of isotype controls. Dead cells were detected using 7-amino-actinomycin D (Via-Probe; BD Pharmingen).

Apoptosis assay

Neutrophils (hESC-Neu's and PB-Neu's) were suspended in IMDM with 0.5% BSA and incubated in 6-well plates at 37°C with 5% CO_2, with or without 50 ng/mL G-CSF. At the indicated time, neutrophils were harvested, stained with FITC-conjugated Annexin V and propidium iodide (PI) using an Annexin V-FITC Kit (Beckman Coulter), and analyzed by FACS Aria. Cells negative for both Annexin V and PI were judged as live cells.

G-CSF stimulation prior to assessing neutrophil function

Because the functions of hESC-Neu's are modified by G-CSF in the culture medium, we stimulated hESC-Neu's and PB-Neu's (PB-Neu(G+)'s) for 15 minutes at 37°C with 50 ng/mL G-CSF in the reaction medium. As a control, PB-Neu's without G-CSF stimulation (PB-Neu(G−)'s) were prepared. hESC-Neu's, PB-Neu(G+)'s, and PB-Neu(G−)'s were used for functional assays directly without changing the medium.

Detection of reactive oxygen species produced by neutrophils

Neutrophil production of reactive oxygen species was detected by flow cytometry using dihydrorhodamine123 (DHR; Sigma-Aldrich, St Louis, MO) as described previously.[20-22] Briefly, 1×10^5 hESC-Neu's, PB-Neu(G+)'s, or PB-Neu(G−)'s were suspended in 400 μL of the reaction medium (HBSS containing 0.5% BSA) per tube, and 3 tubes were prepared of each sample. Catalase (Sigma-Aldrich) at a final concentration of 1000 U/mL, 1.8 μL 29 mM DHR, and 100 μL 3.2 μM phorbol myristate

acetate (PMA; Sigma-Aldrich) were added to 1 of the 3 tubes; either no DHR or only DHR was added in the other 2 tubes as controls. Reaction medium was added to bring the final volume up to 500 μL. After 15-minute reaction at 37°C, the samples were washed twice with ice-cold reaction medium, and suspended in 200 μL reaction medium. Rhodamine fluorescence from the oxidized DHR was detected using FACS Aria.

Phagocytosis and NBT-reduction test using NBT-coated yeast cells

Phagocytosis and NBT reduction were visualized in a single set of experiments. Autoclaved Baker yeast was suspended in 0.5% NBT solution (0.5% NBT [Sigma-Aldrich] and 0.85% sodium chloride in distilled water) at a density of 1×10^8/mL. A 5-μL aliquot of this yeast suspension was added to hESC-Neu's, PB-Neu(G+)'s, and PB-Neu(G−)'s at 2.5×10^5 in 50 μL FBS. After 1 hour at 37°C, the samples were washed and stained with 1% safranin-O (MUTO PURE CHEMCALS) for 5 minutes. The samples were then washed twice and suspended in 100 μL PBS. A small aliquot of each sample was placed onto a glass slide and topped with a cover glass, and the number of ingested yeast cells and their change in color from brown to purple or black were examined using a microscope. Ingested yeast cells that changed color in the cells were counted as NBT-reaction positive, whereas those that were ingested but did not change color were counted as NBT-reaction negative. The phagocytosis rate was calculated as the percentage of neutrophils that contained one or more NBT-positive yeast cells. The phagocytosis score was calculated as the total number of positive yeast cells in 100 neutrophils. Only morphologically determined neutrophils were scored, excluding contaminating cells such as macrophages, the percentage of which was less than 15% of the total cells.

Bacterial killing assay

The bacterial killing assay was performed using *Escherichia coli* ATCC25922 as previously described[23] with some modifications. Briefly, 1×10^8 colony-forming units (CFUs) of exponentially growing bacteria were suspended in 1 mL HEPES-buffered saline with 10% human AB serum (MP Biomedicals, Irvine, CA) and opsonized at 37°C for 30 minutes. Neutrophils (hESC-Neu's, PB-Neu(G−)'s, and PB-Neu(G+)'s) were suspended in HEPES-buffered saline with 40% human AB serum at a concentration of 5×10^6/mL. The opsonized *E coli* was added to the suspension of hESC-Neu's and PB-Neu's, at a neutrophil/bacteria ratio of 2:1, or control medium. After 1-hour incubation, 50 μL of samples with and without neutrophils were diluted in 2.5 mL alkalinized water (pH 11) for lysis of neutrophils. Samples were further diluted with PBS, and duplicate aliquots were added to molten tryptic soy broth with 1.5% agar kept at 42°C, rapidly mixed, and plated on dishes. The CFUs were counted after overnight incubation.

Chemotaxis assay

Chemotactic ability was determined using a modified Boyden chamber method.[24] Briefly, 700 μL of the reaction medium (HBSS containing 0.5% BSA) with or without 10^{-7} M formyl-Met-Leu-Phe (fMLP; Sigma-Aldrich) was placed into each well of a 24-well plate, and the cell culture insert (3.0-μm pores; Falcon; Becton Dickinson, Franklin Lakes, NJ) was gently placed into each well to divide the well into upper and lower sections. Neutrophils were suspended in the reaction medium at 2.5×10^6/mL and 200 μL cell suspension was added to the upper well, allowing the neutrophils to migrate from the upper to the lower side of the membrane for 90 minutes at 37°C. After incubation, the membranes were washed, fixed with methanol, stained with Carrazi hematoxylin (MUTO PURE CHEMICALS), and mounted on the slide glass. The number of neutrophils that migrated through the membrane from the upper to the lower side was counted using a microscope with a high-power lens (× 400) in 3 fields: 2 near the edge and 1 on the center. Only mature neutrophils were counted.

Statistical analyses

Results are expressed as mean plus or minus SD. Statistical significance was determined using a 2-tailed Student *t* test. Results were considered significant when *P* values were less than .05.

Results

Effective derivation of mature neutrophils from hESCs with high purity

After initiating the suspension culture of EB-derived cells, small clusters of round-shaped cells appeared on the OP9 stromal layer around day 4. The morphology of the day-7 cells visualized with Wright-Giemsa staining suggested that they were myeloblasts and promyelocytes. On days 9 and 11, myelocytes and metamyelocytes were predominant, and on day 13 or 14, 70% to 80% of the cells appeared to be stab and segmented neutrophils (Figure 1A), with approximately 90% of the granulocytes at the metamyelocyte stage or later (Table 1). This finding indicated that hESC-derived cells differentiated into mature neutrophils by a process similar to physiologic granulopoiesis. The remaining cells appeared to be macrophages or monocytes, and cells of other lineages, such as erythroid or lymphoid cells, were not observed at any time during the culture. The number of total cells peaked around days 9 to 11, with an average 2.9-fold increase (range; 0.5- to 10.0-fold in 23 independent cultures) compared with the initial EB-derived cell number. The final yield of the cells on day 13 or 14 was 1.7-fold (range; 0.1- to 8.8-fold in 28 independent cultures). We attempted to further purify the hESC-derived mature neutrophils from the "hESC-Neu" population using density gradient methods, but higher purification could not be achieved without massively reducing the cell yield. We therefore used hESC-Neu's in the subsequent experiments.

Most (97.3% ± 1.5%) of the hESC-derived mature neutrophils defined by Wright-Giemsa staining were positive for myeloperoxidase, and the alkaline-phosphatase score of hESC-Neu's was 284 plus or minus 8.6 (Figure 1B). Under transmission electron microscopy, segmented nuclei and round cytoplasmic granules of hESC-Neu's appeared very similar to those in PB-Neu's (Figure 1C).

Some myeloid cell lines, such as HL-60, have abnormal biosynthesis of secondary granule proteins.[25,26] Thus, it is important to verify the biosynthesis of secondary granule proteins in hESC-Neu's. The levels of lactoferrin mRNA in hESC-derived cells at different stages were compared with those in PB-Neu's and BM-MNCs by semiquantitative RT-PCR (Figure 1D). Lactoferrin biosynthesis begins at the myelocyte stage and terminates by the beginning of the band stage.[25,27] Lactoferrin mRNA was not detected in PB-Neu's from some donors, but was detected in PB-Neu's from others. Human ESC–derived cells at various stages as well as BM-MNCs expressed lactoferrin mRNA. The expression level of lactoferrin mRNA in the hESC-derived cells was highest at day 10 of the induction culture and declined on days 13 and 14. These findings are consistent with the documented pattern of lactoferrin biosynthesis.

Surface antigen presentation in comparison to PB-Neu's

Surface antigen expression at each level of differentiation of hESC-derived cells was analyzed by flow cytometry (Figure 2). From days 7 to 13, the common blood cell antigen CD45 was expressed in almost all the cells. CD34, CD117, and CD133, cell surface markers on normal immature hematopoietic cells, were detected in a small population of the cells on day 7, but disappeared by day 10. Common myeloid antigens CD33 and CD15 were also highly expressed, whereas CD11b expression increased during the course of maturation. CD13 is also a common myeloid antigen, but

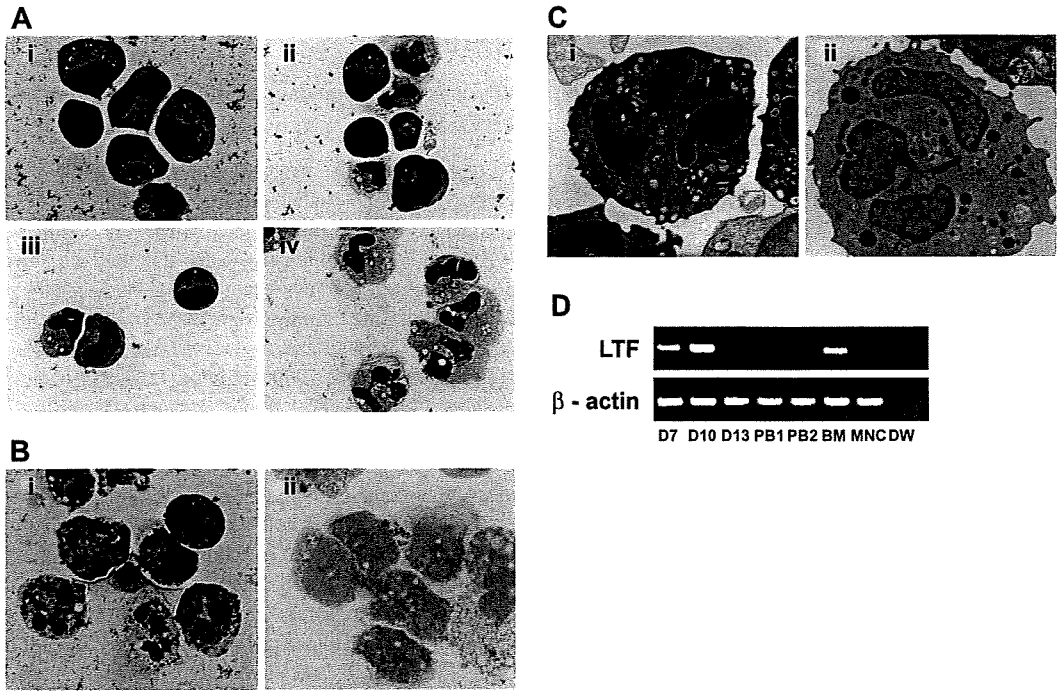

Figure 1. Morphology of hESC-derived cells and expression of lactoferrin mRNA. (A) Wright-Giemsa staining of the day-7 cells (i) revealed that they were morphologically myeloblasts and promyelocytes. On days 9 (ii) and 11 (iii), myelocytes and metamyelocytes were predominant, and on day 13 (iv; hESC-Neu), 70% to 80% of the cells appeared to be stab and segmented neutrophils. Original magnification, ×1000. (Bi) 97.3% plus or minus 1.5% of hESC-Neu's were myeloperoxidase positive. (ii) The neutrophil alkaline-phosphatase score in hESC-Neu's was 284 plus or minus 8.6. Values represent mean plus or minus SD. Original magnification, ×1000. (C) Microstructure of hESC-Neu's. Similar to steady-state neutrophils separated from peripheral blood (i), segmented nuclei and cytoplasmic granules were observed in hESC-Neu's (ii). Original magnification, ×8000. (D) Lactoferrin (LTF) mRNA was expressed in hESC-derived cells on day 7 (D7), peaked on day 10 (D10), and was weakly positive on day 13 (D13). Bone marrow mononuclear cells (BM) were strongly positive for LTF mRNA, but PB-Neu's (PB1 and 2) were negative, although faint bands were detected in PB-Neu's prepared from some donors (data not shown). As a negative control, peripheral blood mononuclear cells (MNCs) were used.

its expression was observed in less than 20% of the cells on day 7 and did not subsequently increase. CD16 (Fcγ receptor (FcγR) III), which is expressed in neutrophils as well as natural killer cells, macrophages, and a small subset of monocytes,[28] was already expressed by day 7, and increased with maturation. This expression pattern of CD16 is consistent with that during normal neutrophil differentiation, although the proportion of $CD16^+$ cells was lower than that of morphology-defined mature neutrophils on day 13. The ratio of CD32 (FcγRII)–positive cells increased as the differentiation stage advanced, and eventually reached 90%. CD64 (FcγRI) expression was greater than 80%, peaking on day 10, and the high percentage was maintained through day 13. CD14 was expressed in 20% to 25% of the cells on days 10 and 13.

Table 1. Differentiation pattern of hESC-derived cells

	% of total cells		
Cell type	Day 7	Day 10	Day 13
Myeloblasts	61.0 ± 9.1	2.3 ± 1.2	ND
Promyelocytes	16.8 ± 6.3	8.5 ± 0.9	0.7 ± 0.8
Myelocytes	12.3 ± 4.8	34.0 ± 6.8	6.4 ± 3.4
Metamyelocytes	3.0 ± 1.0	19.0 ± 1.3	10.2 ± 4.3
Stab neutrophils	0.8 ± 0.3	16.2 ± 3.0	18.3 ± 2.6
Segmented neutrophils	0.3 ± 0.6	14.7 ± 6.0	53.1 ± 9.6
Macrophage/monocytes	5.7 ± 0.6	5.3 ± 1.3	11.2 ± 1.4
Mature neutrophils	1.2 ± 0.8	30.8 ± 4.6	71.4 ± 7.4

The sum of the stab and segmented neutrophils indicates the total mature neutrophils. Data are shown as mean plus or minus SD (n = 3 independent experiments).

ND indicates not detectable.

In normal peripheral blood, both neutrophils and monocytes express CD15 and CD11b. In addition, mature neutrophils express CD16, whereas monocytes express CD14.[28,29] Detailed analysis on day 13 revealed that approximately 70% of $CD15^+$ and $CD11b^+$ cells were $CD16^+$, and almost all $CD15^+$ and $CD16^+$ cells expressed CD11b (Figure 2Bi,ii). Given that 70% to 80% of the cells on day 13 were morphologically mature neutrophils (Table 1), it is likely that the majority of hESC-Neu's had CD15, CD11b, and CD16 expression patterns similar to PB-Neu's, although some hESC-Neu's did not express CD15 or CD16, particularly CD16.

CD32 is broadly expressed on myeloid cells, whereas CD64 is expressed only on monocytes but not on neutrophils in the peripheral blood.[28] In the bone marrow, CD64 expression is observed in a small population of myeloblasts, peaks at the promyelocyte, myelocyte, and metamyelocyte stages, and then diminishes, although a small proportion of the stab neutrophils still express CD64.[30,31] We confirmed that virtually no PB-Neu's expressed CD64 (data not shown). In contrast, almost all $CD15^+$ and $CD16^+$ hESC-Neu's expressed CD64 on day 13, indicating that both stab and segmented hESC-Neu's expressed CD64, because segmented neutrophils represented more than 50% of the cells on day 13 (Figure 2Biii; Table 1). Nearly 50% of $CD15^+$ and $CD16^+$ cells were weakly positive for CD14, in contrast to the negative expression of CD14 in steady-state PB-Neu's (Figure 2Biv). This aberrant expression of CD64 and CD14 in hESC-Neu's is similar to their positive expression on some of the neutrophils harvested from healthy donors who received G-CSF administration[32,33] and the neutrophils derived from bone marrow $CD34^+$ cells in vitro by G-CSF stimulation.[31]

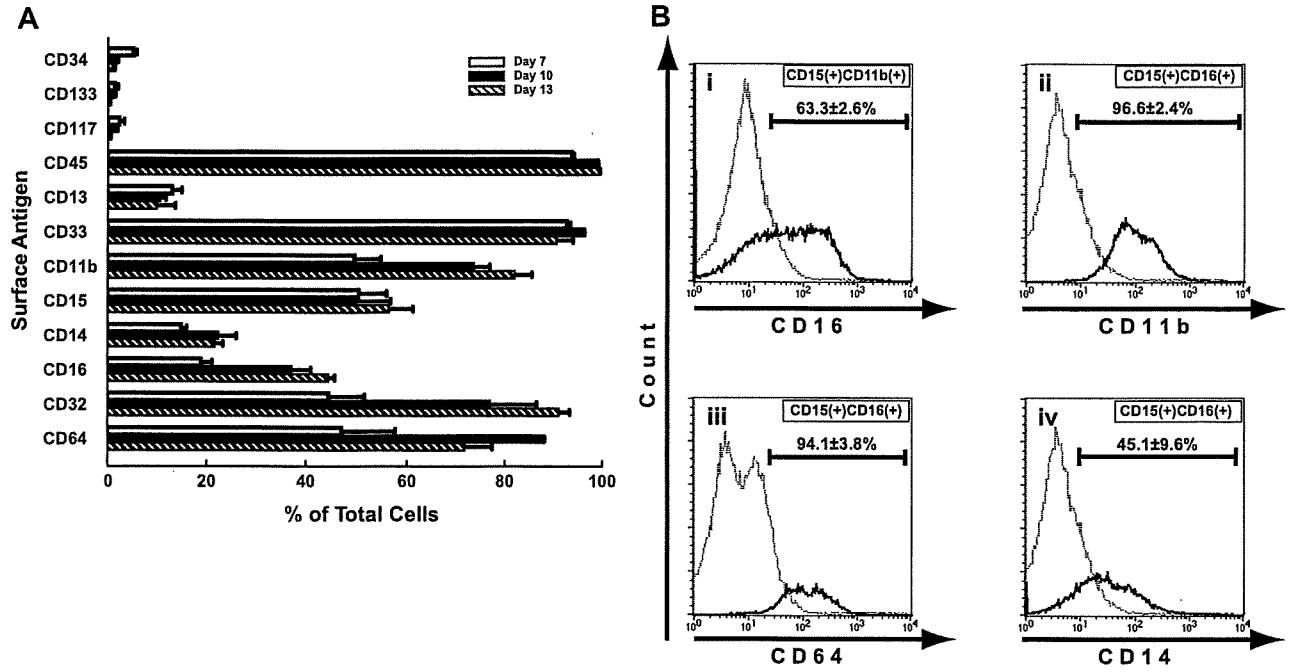

Figure 2. Surface antigens of hESC-derived cells. (A) Surface antigen expression at each level of differentiation of hESC-derived cells was analyzed by flow cytometry. CD45 was expressed in almost all the cells. CD34, CD117, and CD133, immature markers of hematopoiesis, were detected in a small population of the cells on day 7, and had almost disappeared by day 10. Common myeloid antigens CD33 and CD15 were highly expressed, and the expression of CD11b increased during maturation. CD13 was expressed in less than 20% of the cells throughout the culture period. The expression of CD16, a mature neutrophil marker, increased following maturation, but was observed in only approximately 45% of the cells, even on day 13. CD14 and CD64 expression was aberrantly observed in some cells. Bars represent SDs (n = 3). (B) In the steady state, mature neutrophils in peripheral blood were $CD15^+$, $CD11b^+$, and $CD16^+$. (i) In hESC-derived cells on day 13, 63.3% plus or minus 2.6% of the $CD15^+$ and $CD11b^+$ cells were $CD16^+$, and (ii) almost all of the $CD15^+$ and $CD16^+$ cells were $CD11b^+$. (iii-iv) On the other hand, CD64 and CD14 were rarely expressed on mature neutrophils in the peripheral blood. $CD15^+$ and $CD16^+$ cells from hESCs, consistent with the phenotype of mature neutrophils, showed aberrant expression of CD64 (iii) and CD14 (iv), in 94.1% plus or minus 3.8% and 45.1% plus or minus 9.6% of the cells, respectively. Data are presented as mean plus or minus SD (n = 3).

Apoptosis pattern and prolonged survival by G-CSF of hESC-Neu's and PB-Neu's

In the steady state, PB-Neu's have a short life span of approximately 24 hours, but this can be prolonged by G-CSF stimulation.[34] Some hESC-Neu's were already apoptotic at the time of harvest and therefore we focused on the nonapoptotic fraction of hESC-Neu's (Figure 3). In contrast to the PB-Neu's, which underwent apoptosis within 6 hours without G-CSF, consistent with previous reports,[34] a proportion of apoptotic cells among hESC-Neu's in the medium without G-CSF did not increase for up to 6 hours after the start of the culture. In addition, there were no differences between the cultures with and without G-CSF for up to 6 hours. After 6 hours, however, there was a more rapid decrease in nonapoptotic cells in hESC-Neu's without G-CSF than in hESC-Neu's with G-CSF, which resulted in a lower number of viable cells than hESC-Neu's with G-CSF at 24 hours, although the number of viable cells of hESC-Neu's without G-CSF was still higher than that of PB-Neu's without G-CSF.

Oxidative burst phenotype was similar in hESC-Neu's and PB-Neu's

Oxidative burst is an essential function of neutrophils when killing microorganisms, but an inappropriate burst sometime causes injury to the host tissue. We assessed the ability to convert DHR to rhodamine in hESC-Neu's and PB-Neu's using flow cytometry.[20] Because G-CSF, which could substantially affect the result, was used during the culture, we compared hESC-Neu's with PB-Neu(G+)'s and PB-Neu(G−)'s as described in "G-CSF stimulation prior to assessing neutrophil function." When DHR was added to the neutrophil suspensions, rhodamine-specific fluorescence was detected in hESC-Neu's, and in PB-Neu(G−)'s and PB-Neu(G+)'s without PMA stimulation, indicating basal superoxide production without PMA stimulation in each neutrophil preparation (Figure 4). PMA stimulation increased rhodamine mean fluorescence intensity in hESC-Neu's, but to a lesser extent than in PB-Neu(G−)'s and PB-Neu(G+)'s. Consequently, the mean rhodamine fluorescence intensity after PMA stimulation was similar in hESC-Neu's, PB-Neu(G−)'s, and PB-Neu(G+)'s, suggesting that the maximum superoxide production is comparable between hESC-Neu's and PB-Neu's.

Phagocytosis and subsequent NBT reduction activity, and bactericidal activity were similar between hESC-Neu's and PB-Neu's

Neutrophils protect against infectious microorganisms by phagocytosing and subsequently killing them. These functions of hESC-Neu's and PB-Neu's were evaluated in an experimental system using NBT-coated yeast. Under the microscope, mature neutrophils could be easily distinguished from contaminating macrophages by the unique shape of their nuclei after 1% safranin-O staining (Figure 5A). NBT-coated yeast that had not been ingested had a red-brown color that began to change to purple or black, beginning at the periphery, and eventually became completely black, because the NBT coating on the yeast was reduced by neutrophils after phagocytosis. Thus, neutrophils that had phagocytosis and NBT-reducing ability could be easily identified. hESC-Neu's had a slightly lower phagocytosis rate than PB-Neu(G−)'s and PB-Neu(G+)'s (Figure 5B). The phagocytosis score, however, was not significantly different between hESC-Neu's and PB-Neu(G−)'s and PB-Neu(G+)'s (Figure 5C). The cells on day 8 of the culture, most of which were morphologically myeloblasts and promyelocytes, were rarely observed

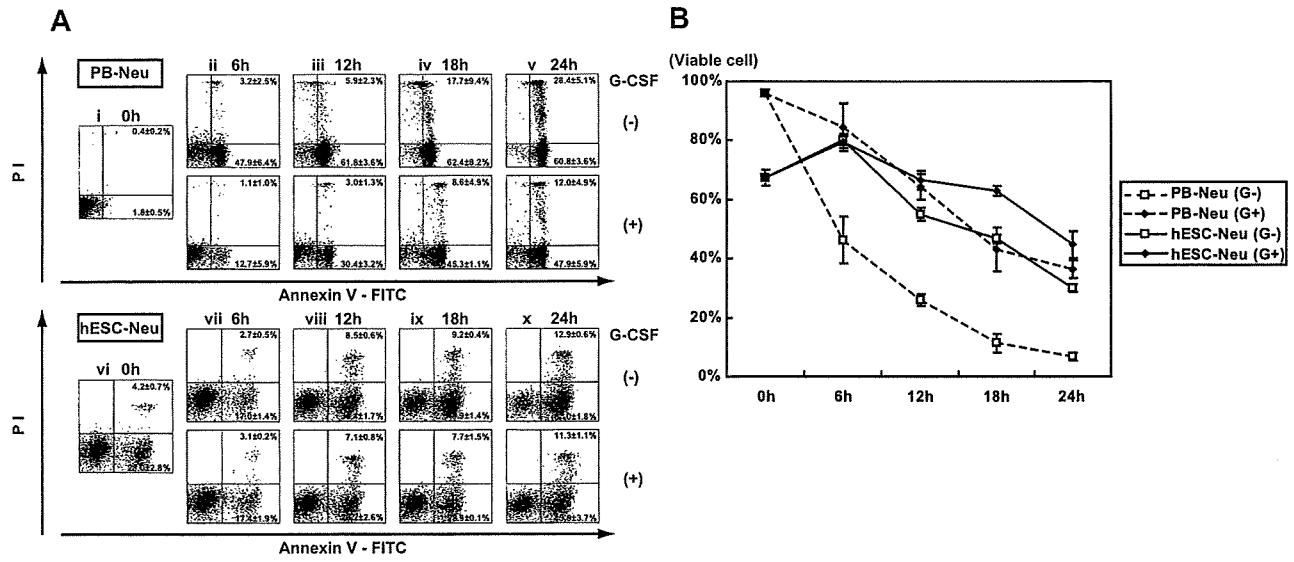

Figure 3. Apoptosis pattern and G-CSF effect on survival of hESC-Neu's. (A) Flow cytometric analysis. In the steady state, PB-Neu's have a short life span of approximately 24 hours, but this can be prolonged by G-CSF stimulation (i-v). Some hESC-Neu's were already apoptotic at the time of the harvest from the induction culture (vi). In contrast to the PB-Neu's that underwent apoptosis within 6 hours without G-CSF (ii), the proportion of apoptotic cells did not increase for up to 6 hours after the start of the culture of hESC-Neu's in the medium without G-CSF (vi,vii). In addition, there were no differences between the cultures of hESC-Neu's with and without G-CSF for up to 6 hours (vii). After 6 hours, nonapoptotic cells decreased more rapidly among hESC-Neu's without G-CSF than among hESC-Neu's with G-CSF (viii-x), resulting in the lower number of viable cells than hESC-Neu's with G-CSF at 24 hours (x). Figures are representative of 3 independent experiments. Data are presented as mean plus or minus SD (n = 3). (B) The time course of the decrease in viable cells. Bars represent SDs (n = 3).

to phagocytose the yeast or reduce NBT if they had ingested the yeast, indicating that we observed phagocytosis and NBT reduction that was specific to mature neutrophils.

Because the hESC-Neu's had sufficient phagocytosing ability and superoxide production, we next investigated whether hESC-Neu's can kill bacteria. The bactericidal activity of hESC-Neu's and PB-Neu's was compared using *E coli*. When incubated with hESC-Neu's and PB-Neu(G−)'s and PB-Neu(G+)'s, the numbers of CFUs were similarly reduced to approximately 40% that of the control, indicating comparable bactericidal activity against *E coli* between hESC-Neu's and PB-Neu's (Figure 5D).

Chemotaxis was similar between hESC-Neu's and PB-Neu's

We compared chemotaxis of hESC-Neu's and PB-Neu's using a modified Boyden chamber method. After incubation with or without fMLP in the lower well, neutrophils had migrated from the upper side to the lower side of the membrane. Neutrophil migration without fMLP in the lower well was considered random migration. The number of neutrophils that migrated randomly was not significantly different between hESC-Neu's and PB-Neu(G−)'s, but PB-Neu(G+)'s showed significantly more random migration than the others (Figure 5E). The number of migrated cells increased in hESC-Neu's, PB-Neu(G−)'s, and PB-Neu(G+)'s when fMLP was added in the lower well. The increase in cell migration induced by chemotaxis to fMLP was calculated by subtracting the number of randomly migrated cells without fMLP from that of migrated cells with fMLP. There were no significant differences between hESC-Neu's and PB-Neu(G−)'s or PB-Neu(G+)'s in the net fMLP-induced chemotaxis.

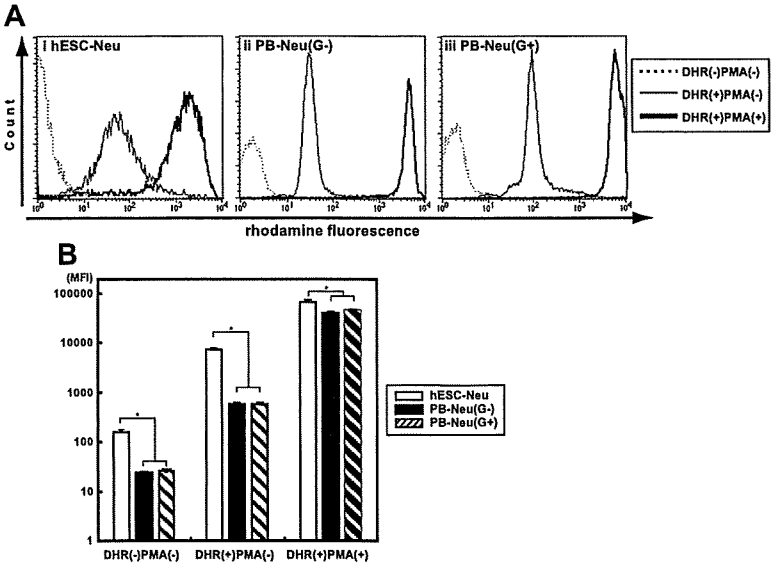

Figure 4. Superoxide production of hESC-Neu's assessed by dihydrorhodamine123 oxidation. (A) Dihydrorhodamine123 (DHR) was reacted to neutrophils with or without phorbol myristate acetate (PMA), and the resultant rhodamine fluorescence was detected by flow cytometry. When DHR was added to the reaction medium without PMA (line), the fluorescence levels were slightly elevated in hESC-Neu's (i), PB-Neu(G−)'s (ii), and PB-Neu(G+)'s (iii). The addition of PMA dramatically increased the levels of fluorescence in all 3 neutrophil preparations (bold line). The figures are representative of 3 independent experiments. (B) Comparison of superoxide production between hESC-Neu's and PB-Neu's using mean fluorescence intensity (MFI) of rhodamine. When DHR was added without PMA stimulation, rhodamine-specific fluorescence was detected in hESC-Neu's, PB-Neu(G−)'s, and PB-Neu(G+)'s. PMA stimulation increased rhodamine MFI in hESC-Neu's though to a lesser extent than in PB-Neu(G−)'s and PB-Neu(G+)'s. Consequently, rhodamine MFI after PMA stimulation was similar in hESC-Neu's, PB-Neu(G−)'s, and PB-Neu(G+)'s, suggesting that the maximum superoxide production was comparable between hESC-Neu's and PB-Neu's (n = 3; bars represent SDs; $^*P < .05$ compared with hESC-Neu's).

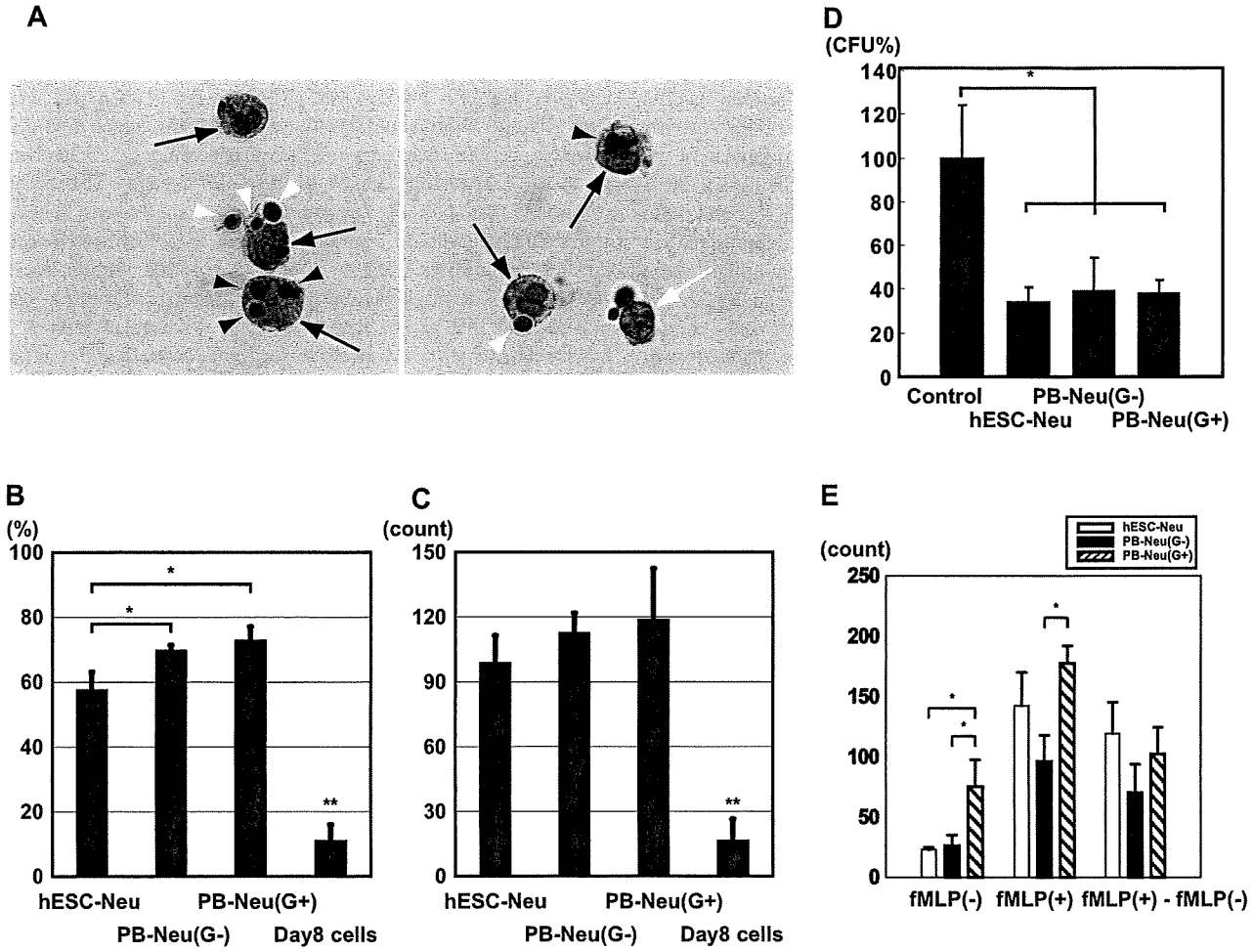

Figure 5. NBT-coated yeast cell-phagocytosis test, bactericidal activity, and chemotaxis assay. (A) NBT-coated yeast cells were added to a neutrophil suspension and incubated at 37°C. After 1 hour, the cells were stained with 1% safranin-O, and observed using a microscope. Mature neutrophils (→) could be easily distinguished from contaminating macrophages (white arrow; only the nucleus is observed in the figure) by the unique shape of their nuclei. Yeast cells were red-brown in color before being ingested (white arrowhead); the color began to change to purple or black beginning at the periphery of the yeast cell, and eventually became completely black (➤) because the NBT was reduced after ingestion. Yeast cells that changed color in the cells were counted as NBT-reduction positive. Original magnification, ×400. (B) The phagocytosis rate was calculated as a percentage of the neutrophils that contained one or more yeast cells. hESC-Neu's had a slightly lower phagocytosis rate than that of PB-Neu(G−)'s and PB-Neu(G+)'s. (C) The phagocytosis score was calculated as the total number of positive yeast cells in 100 neutrophils. There were no significant differences in the phagocytosis score between hESC-Neu's and PB-Neu(G−)'s or PB-Neu(G+)'s. The cells on day 8 of the culture (day-8 cells) were rarely observed to phagocytose the yeast cells or reduce NBT. (In B-C, n = 3; bars indicate SDs; $^*P < .05$ compared with PB-Neu(G−)'s and PB-Neu(G+)'s; $^{**}P < .05$ compared with hESC-Neu's, PB-Neu(G−)'s, and PB-Neu(G+)'s.) (D) Bactericidal assay. *E coli* was opsonized with human AB serum, and incubated with hESC-Neu's, PB-Neu(G−)'s, PB-Neu(G+)'s, or control medium. After 1-hour incubation with hESC-Neu's, PB-Neu(G−)'s, and PB-Neu(G+)'s, the colony-forming units (CFUs) were significantly reduced to approximately 40% of the control. There were no significant differences in bactericidal activity between hESC-Neu's, PB-Neu(G−)'s, and PB-Neu(G+)'s. The CFUs of controls are presented as 100% (n = 3; bars indicate SDs; $^*P < .05$ compared with control). (E) Chemotaxis assay by a modified Boyden chamber method. The number of neutrophils that migrated randomly (fMLP(−)) was not significantly different between hESC-Neu's and PB-Neu(G−)'s, but PB-Neu(G+)'s showed significantly greater random migration than hESC-Neu's and PB-Neu(G−)'s. The number of migrating cells increased in all hESC-Neu's, PB-Neu(G−)'s, and PB-Neu(G+)'s when fMLP was added to the lower well (fMLP(+)). The increase in the number of migrating cells induced by chemotaxis to fMLP (fMLP(+)-fMLP(−)) was not significantly different between hESC-Neu's and PB-Neu(G−)'s or PB-Neu(G+)'s (n = 3; bars indicate SDs; $^*P < .05$).

Discussion

We developed a specific and effective method for deriving mature neutrophils from hESCs, making it possible to analyze hESC-derived neutrophils in detail. hESC-derived neutrophils had characteristics similar to steady-state peripheral blood mature neutrophils in morphology and essential functions, although there were some differences in surface antigen expression.

Unfortunately, attempts to further purify the hESC-derived mature neutrophils from the hESC-Neu population by density gradient methods led to a massive reduction in cell yield. In the flow cytometric analysis, the mean intensity of hESC-Neu's in forward scatter was higher than that of PB-Neu's (data not shown), indicating that the size of morphologically mature neutrophils, comprising 70% to 80% of the hESC-Neu population, was larger than that of PB-Neu's. This finding indicates that the density of morphologically mature neutrophils in the hESC-Neu population was lower than that of PB-Neu's, which made it difficult to separate hESC-Neu's from other contaminating cells.

In this culture, we observed morphologically defined myeloblasts, promyelocytes, myelocytes, metamyelocytes, and, eventually, mature stab and segmented neutrophils, in this order, during the 13-day culture, which is similar to the granulocyte maturation process in bone marrow. The surface antigen expression pattern during differentiation was similar to that during normal granulopoiesis, with CD34 and CD117 expression on immature cells, and an increase in CD16 expression as differentiation advanced. Most

hESC-Neu's expressed CD16, CD15, CD11b, CD33, and CD45. This pattern is consistent with normal PB-Neu's, but the percentage of CD16-expressing cells was lower than that of mature neutrophils determined by morphology. The lower CD16 expression level is documented in neutrophils derived in vitro from bone marrow $CD34^+$ cells by stimulation with G-CSF, and is considered to be the effect of G-CSF on myeloid progenitors.[31] G-CSF also induces CD64 and CD14 expression on mature neutrophils,[31,35] and these effects are also observed in vivo when G-CSF is administered to healthy volunteers.[32,33] Therefore, the G-CSF present in the culture from day 7 may have affected the progenitors and led to the relatively low expression of CD16 on hESC-Neu's and aberrant expression of CD64 and CD14 on $CD15^+$ and $CD16^+$ hESC-Neu's.

In the apoptosis assay, some hESC-Neu's were already apoptotic at the time of the harvest from the induction culture, but the proportion of apoptotic cells among hESC-Neu's in the medium without G-CSF did not increase for up to 6 hours after the start of the culture. There are 2 possible reasons for the difference in the rate of apoptosis. First, the hESC-Neu's were more heterogeneous than the PB-Neu's, as they comprised cells at different stages from incompletely differentiated cells such as metamyelocytes to maturation-completed and aged neutrophils. Relatively immature cells or unaged mature neutrophils in the hESC-Neu population might have a longer lifespan than PB-Neu's. Second, the effect of G-CSF used in the induction culture might continue even after the washout.

In the chemotaxis assay, the random migration of hESC-Neu's was almost the same as that of PB-Neu(G−)'s, but lower than that of PB-Neu(G+)'s, although hESC-Neu's were stimulated by G-CSF before the assay. The effect of G-CSF on the random migration of neutrophils is controversial; random migration increases in vitro when neutrophils are stimulated by G-CSF,[36] whereas neutrophils obtained from G-CSF–treated patients with nonmyeloid malignancies show decreased random migration and chemotaxis.[37,38] Our in vitro experiment with PB-Neu(G+)'s and PB-Neu(G−)'s replicated the former result. Nevertheless, hESC-Neu's showed relatively low random migration despite stimulation with G-CSF, while maintaining almost normal fMLP-induced chemotaxis. One possible reason for these differences might be the continuous stimulation by G-CSF; hESC-Neu's were stimulated from the myeloblast stage, and thus, it was expected that the characteristics of the hESC-Neu's were more similar to those of neutrophils from G-CSF–stimulated donors rather than to normal mature neutrophils.

The low yield of hESC-Neu's is a major obstacle to their functional analysis in animals, and further, to their potential use in drug screening and clinical applications. The number of hESC-Neu's produced was less than twice that of the input EB-derived cells. Recently, erythroid progenitor cell lines that could differentiate into functional mature red blood cells both in vitro and in vivo were established from mouse ESCs.[39] In that report, the starting number of ESCs required to establish one progenitor line was 5×10^5, and transplantation of 2×10^7 cells of the progenitor line could ameliorate anemia in mice by increasing the red blood cell count. Similar methods could be considered in the granulopoiesis from hESCs. Another potential method is to use more immature or proliferation-competent cells than the cells with which we initiated the induction culture. One candidate may be hematopoietic progenitors that emerge in saclike structures derived from ESCs. In a report using cynomolgus monkey ESCs,[40] EBs were created and subsequently subjected to adherent culture on a gelatin-coated dish. After 2 weeks, saclike structures emerged that contained hematopoietic precursors at various stages of myeloid lineage. The authors mentioned the possible existence of hemangioblasts, because endothelial cells could be produced from those precursors under different conditions. Others have also reported similar saclike structures containing hematopoietic precursors created from hESCs.[10] In this paper, megakaryocytes were created from the inner cells, which were positive for hematoendothelial markers, such as CD34, CD31, vascular endothelial growth factor-receptor 2, and vascular endothelial-cadherin. These similar findings suggest that the cells in the saclike structures contain cells that are more immature than our EB-derived cells, and that the precursors inside the saclike structures have greater proliferation potency than our EB-derived cells. Because neither paper directly demonstrated the efficiency of mature blood cell production from monkey or human ES cells, however, the efficiency of producing neutrophils from our EB-derived cells should be compared with that from the saclike structure–derived cells.

Acknowledgments

We thank Dr Nakatsuji for providing the KhES-3, and Dr Nakano for providing the OP9 cells. We are grateful to Kyowa Hakko Kirin for providing TPO, FP6, and G-CSF, and to Kyokuto Pharmaceutical Industrial for the nonserum medium used in the EB formation. We also thank S. Ichimura for hESC culture.

This work was supported in part by a Grant-in-aid from the Japan Society of Promotion of Sciences (KAKENHI nos. 17390274, 18013012, 19390258, and 20015010); Research on Pharmaceutical and Medical Safety, Health and Labor Sciences Research Grants from the Ministry of Health, Labor and Welfare of Japan (H16-Iyaku-32); grants from the Astellas Foundation for Research on Metabolic Disorders; the Uehara Memorial Foundation; and the Sagawa Foundation for Promotion of Cancer Research (S.C.); and the Project for Realization of Regenerative Medicine (S.O.).

Authorship

Contribution: Y.Y. and T.S. performed the experiments; K.H. designed the NBT-coated yeast cell-phagocytosis test; M.S.-Y., and K.K. assisted with interpretation of experiments and provided insightful comments; Y.Y. interpreted the data, made the figures, and wrote the paper; T.T., M.K., and S.O. advised on experimental design; S.C. provided critical reading of the paper; T.S. and S.C. designed the research.

Conflict-of-interest disclosure: The authors declare no competing financial interests.

Correspondence: Shigeru Chiba, Department of Clinical and Experimental Hematology, University of Tsukuba, 1-1-1 Tennodai, Tsukuba, Ibaraki, 305-8575, Japan; e-mail: schiba-tky@umin.net.

References

1. Kaufman DS, Hanson ET, Lewis RL, Auerbach R, Thomson JA. Hematopoietic colony-forming cells derived from human embryonic stem cells. Proc Natl Acad Sci U S A. 2001;98:10716-10721.
2. Nakano T, Kodama H, Honjo T. Generation of lymphohematopoietic cells from embryonic stem cells in culture. Science. 1994;265:1098-1101.
3. Vodyanik MA, Bork JA, Thomson JA, Slukvin II. Human embryonic stem cell-derived CD34+ cells: efficient production in the coculture with OP9 stromal cells and analysis of lymphohematopoietic potential. Blood. 2005;105:617-626.

4. Chadwick K, Wang L, Li L, et al. Cytokines and BMP-4 promote hematopoietic differentiation of human embryonic stem cells. Blood. 2003;102: 906-915.
5. Cerdan C, Rouleau A, Bhatia M. VEGF-A165 augments erythropoietic development from human embryonic stem cells. Blood. 2004;103: 2504-2512.
6. Wang L, Menendez P, Shojaei F, et al. Generation of hematopoietic repopulating cells from human embryonic stem cells independent of ectopic HOXB4 expression. J Exp Med. 2005;201:1603-1614.
7. Keller G, Kennedy M, Papayannopoulou T, Wiles MV. Hematopoietic commitment during embryonic stem cell differentiation in culture. Mol Cell Biol. 1993;13:473-486.
8. Wang L, Li L, Shojaei F, et al. Endothelial and hematopoietic cell fate of human embryonic stem cells originates from primitive endothelium with hemangioblastic properties. Immunity. 2004;21: 31-41.
9. Lu SJ, Feng Q, Caballero S, et al. Generation of functional hemangioblasts from human embryonic stem cells. Nat Methods. 2007;4:501-509.
10. Takayama N, Nishikii H, Usui J, et al. Generation of functional platelets from human embryonic stem cells in vitro via ES-sacs, VEGF-promoted structures that concentrate hematopoietic progenitors. Blood. 2008;111:5298-5306.
11. Hübel K, Carter RA, Liles WC, et al. Granulocyte transfusion therapy for infections in candidates and recipients of HPC transplantation: a comparative analysis of feasibility and outcome for community donors versus related donors. Transfusion. 2002;42:1414-1421.
12. Mousset S, Hermann S, Klein SA, et al. Prophylactic and interventional granulocyte transfusions in patients with haematological malignancies and life-threatening infections during neutropenia. Ann Hematol. 2005;84:734-741.
13. Price TH. Granulocyte transfusion: current status. Semin Hematol. 2007;44:15-23.
14. Bhatia M. Hematopoietic development from human embryonic stem cells. Hematology Am Soc Hematol Educ Program. 2007;2007:11-16.
15. Suemori H, Yasuchika K, Hasegawa K, Fujioka T, Tsuneyoshi N, Nakatsuji N. Efficient establishment of human embryonic stem cell lines and long-term maintenance with stable karyotype by enzymatic bulk passage. Biochem Biophys Res Commun. 2006;345:926-932.
16. Thomson JA, Itskovitz-Eldor J, Shapiro SS, et al. Embryonic stem cell lines derived from human blastocysts. Science. 1998;282:1145-1147.
17. Suzuki T, Yokoyama Y, Kumano K, et al. Highly efficient ex vivo expansion of human hematopoietic stem cells using Delta1-Fc chimeric protein. Stem Cells. 2006;24:2456-2465.
18. Yuo A, Kitagawa S, Okabe T, et al. Recombinant human granulocyte colony-stimulating factor repairs the abnormalities of neutrophils in patients with myelodysplastic syndromes and chronic myelogenous leukemia. Blood. 1987;70:404-411.
19. Kumano K, Chiba S, Shimizu K, et al. Notch1 inhibits differentiation of hematopoietic cells by sustaining GATA-2 expression. Blood. 2001;98:3283-3289.
20. Vowells SJ, Sekhsaria S, Malech HL, Shalit M, Fleisher TA. Flow cytometric analysis of the granulocyte respiratory burst: a comparison study of fluorescent probes. J Immunol Methods. 1995; 178:89-97.
21. Richardson MP, Ayliffe MJ, Helbert M, Davies EG. A simple flow cytometry assay using dihydrorhodamine for the measurement of the neutrophil respiratory burst in whole blood: comparison with the quantitative nitrobluetetrazolium test. J Immunol Methods. 1998;219:187-193.
22. Emmendörffer A, Hecht M, Lohmann-Matthes ML, Roesler J. A fast and easy method to determine the production of reactive oxygen intermediates by human and murine phagocytes using dihydrorhodamine 123. J Immunol Methods. 1990; 131:269-275.
23. Decleva E, Menegazzi R, Busetto S, Patriarca P, Dri P. Common methodology is inadequate for studies on the microbicidal activity of neutrophils. J Leukoc Biol. 2006;79:87-94.
24. Harvath L, Falk W, Leonard EJ. Rapid quantitation of neutrophil chemotaxis: use of a polyvinylpyrrolidone-free polycarbonate membrane in a multiwell assembly. J Immunol Methods. 1980;37: 39-45.
25. Rado TA, Bollekens J, St Laurent G, Parker L, Benz EJ Jr. Lactoferrin biosynthesis during granulocytopoiesis. Blood. 1984;64:1103-1109.
26. Rado TA, Wei XP, Benz EJ Jr. Isolation of lactoferrin cDNA from a human myeloid library and expression of mRNA during normal and leukemic myelopoiesis. Blood. 1987;70:989-993.
27. Cowland JB, Borregaard N. The individual regulation of granule protein mRNA levels during neutrophil maturation explains the heterogeneity of neutrophil granules. J Leukoc Biol. 1999;66:989-995.
28. van de Winkel JG, Anderson CL. Biology of human immunoglobulin G Fc receptors. J Leukoc Biol. 1991;49:511-524.
29. van Lochem EG, van der Velden VH, Wind HK, te Marvelde JG, Westerdaal NA, van Dongen JJ. Immunophenotypic differentiation patterns of normal hematopoiesis in human bone marrow: reference patterns for age-related changes and disease-induced shifts. Cytometry B Clin Cytom. 2004;60:1-13.
30. Ball ED, McDermott J, Griffin JD, Davey FR, Davis R, Bloomfield CD. Expression of the three myeloid cell-associated immunoglobulin G Fc receptors defined by murine monoclonal antibodies on normal bone marrow and acute leukemia cells. Blood. 1989;73:1951-1956.
31. Kerst JM, van de Winkel JG, Evans AH, et al. Granulocyte colony-stimulating factor induces hFc gamma RI (CD64 antigen)-positive neutrophils via an effect on myeloid precursor cells. Blood. 1993;81:1457-1464.
32. Kerst JM, de Haas M, van der Schoot CE, et al. Recombinant granulocyte colony-stimulating factor administration to healthy volunteers: induction of immunophenotypically and functionally altered neutrophils via an effect on myeloid progenitor cells. Blood. 1993;82:3265-3272.
33. Carulli G. Effects of recombinant human granulocyte colony-stimulating factor administration on neutrophil phenotype and functions. Haematologica. 1997;82:606-616.
34. van Raam BJ, Drewniak A, Groenewold V, van den Berg TK, Kuijpers TW. Granulocyte colony-stimulating factor delays neutrophil apoptosis by inhibition of calpains upstream of caspase-3. Blood. 2008;112:2046-2054.
35. Kerst JM, Slaper-Cortenbach IC, von dem Borne AE, van der Schoot CE, van Oers RH. Combined measurement of growth and differentiation in suspension cultures of purified human CD34-positive cells enables a detailed analysis of myelopoiesis. Exp Hematol. 1992;20:1188-1193.
36. Nakamae-Akahori M, Kato T, Masuda S, et al. Enhanced neutrophil motility by granulocyte colony-stimulating factor: the role of extracellular signal-regulated kinase and phosphatidylinositol 3-kinase. Immunology. 2006;119:393-403.
37. Azzarà A, Carulli G, Rizzuti-Gullaci A, Minnucci S, Capochiani E, Ambrogi F. Motility of rhG-CSF-induced neutrophils in patients undergoing chemotherapy: evidence for inhibition detected by image analysis. Br J Haematol. 1996;92:161-168.
38. Ribeiro D, Veldwijk MR, Benner A, et al. Differences in functional activity and antigen expression of granulocytes primed in vivo with filgrastim, lenograstim, or pegfilgrastim. Transfusion. 2007; 47:969-980.
39. Hiroyama T, Miharada K, Sudo K, Danjo I, Aoki N, Nakamura Y. Establishment of mouse embryonic stem cell-derived erythroid progenitor cell lines able to produce functional red blood cells. PLoS ONE. 2008;3:e1544.
40. Nakahara M, Matsuyama S, Saeki K, et al. A feeder-free hematopoietic differentiation system with generation of functional neutrophils from feeder- and cytokine-free primate embryonic stem cells. Cloning Stem Cells. 2008;10:341-354.

Vol 459|4 June 2009|doi:10.1038/nature07969

LETTERS

Frequent inactivation of A20 in B-cell lymphomas

Motohiro Kato[1,2], Masashi Sanada[1,5], Itaru Kato[6], Yasuharu Sato[7], Junko Takita[1,2,3], Kengo Takeuchi[8], Akira Niwa[6], Yuyan Chen[1,2], Kumi Nakazaki[1,4,5], Junko Nomoto[9], Yoshitaka Asakura[9], Satsuki Muto[1], Azusa Tamura[1], Mitsuru Iio[1], Yoshiki Akatsuka[11], Yasuhide Hayashi[12], Hiraku Mori[13], Takashi Igarashi[2], Mineo Kurokawa[4], Shigeru Chiba[3], Shigeo Mori[14], Yuichi Ishikawa[8], Koji Okamoto[10], Kensei Tobinai[9], Hitoshi Nakagama[10], Tatsutoshi Nakahata[6], Tadashi Yoshino[7], Yukio Kobayashi[9] & Seishi Ogawa[1,5]

A20 is a negative regulator of the NF-κB pathway and was initially identified as being rapidly induced after tumour-necrosis factor-α stimulation[1]. It has a pivotal role in regulation of the immune response and prevents excessive activation of NF-κB in response to a variety of external stimuli[2–7]; recent genetic studies have disclosed putative associations of polymorphic *A20* (also called *TNFAIP3*) alleles with autoimmune disease risk[8,9]. However, the involvement of A20 in the development of human cancers is unknown. Here we show, using a genome-wide analysis of genetic lesions in 238 B-cell lymphomas, that *A20* is a common genetic target in B-lineage lymphomas. A20 is frequently inactivated by somatic mutations and/or deletions in mucosa-associated tissue lymphoma (18 out of 87; 21.8%) and Hodgkin's lymphoma of nodular sclerosis histology (5 out of 15; 33.3%), and, to a lesser extent, in other B-lineage lymphomas. When re-expressed in a lymphoma-derived cell line with no functional *A20* alleles, wild-type A20, but not mutant A20, resulted in suppression of cell growth and induction of apoptosis, accompanied by downregulation of NF-κB activation. The A20-deficient cells stably generated tumours in immunodeficient mice, whereas the tumorigenicity was effectively suppressed by re-expression of A20. In A20-deficient cells, suppression of both cell growth and NF-κB activity due to re-expression of A20 depended, at least partly, on cell-surface-receptor signalling, including the tumour-necrosis factor receptor. Considering the physiological function of A20 in the negative modulation of NF-κB activation induced by multiple upstream stimuli, our findings indicate that uncontrolled signalling of NF-κB caused by loss of A20 function is involved in the pathogenesis of subsets of B-lineage lymphomas.

Malignant lymphomas of B-cell lineages are mature lymphoid neoplasms that arise from various lymphoid tissues[10,11]. To obtain a comprehensive registry of genetic lesions in B-lineage lymphomas, we performed a single nucleotide polymorphism (SNP) array analysis of 238 primary B-cell lymphoma specimens of different histologies, including 64 samples of diffuse large B-cell lymphomas (DLBCLs), 52 follicular lymphomas, 35 mantle cell lymphomas (MCLs), and 87 mucosa-associated tissue (MALT) lymphomas (Supplementary Table 1). Three Hodgkin's-lymphoma-derived cell lines were also analysed. Interrogating more than 250,000 SNP sites, this platform permitted the identification of copy number changes at an average resolution of less than 12 kilobases (kb). The use of large numbers of SNP-specific probes is a unique feature of this platform, and combined with the CNAG/AsCNAR software, enabled accurate determination of 'allele-specific' copy numbers, and thus allowed for sensitive detection of loss of heterozygosity (LOH) even without apparent copy-number reduction, in the presence of up to 70–80% normal cell contamination[12,13].

Lymphoma genomes underwent a wide range of genetic changes, including numerical chromosomal abnormalities and segmental gains and losses of chromosomal material (Supplementary Fig. 1), as well as copy-number-neutral LOH, or uniparental disomy (Supplementary Fig. 2). Each histology type had a unique genomic signature, indicating a distinctive underlying molecular pathogenesis for different histology types (Fig. 1a and Supplementary Fig. 3). On the basis of the genomic signatures, the initial pathological diagnosis of MCL was re-evaluated and corrected to DLBCL in two cases. Although most copy number changes involved large chromosomal segments, a number of regions showed focal gains and deletions, accelerating identification of their candidate gene targets. After excluding known copy number variations, we identified 46 loci showing focal gains (19 loci) or deletions (27 loci) (Supplementary Tables 2 and 3 and Supplementary Fig. 4).

Genetic lesions on the NF-κB pathway were common in B-cell lymphomas and found in approximately 40% of the cases (Supplementary Table 1), underpinning the importance of aberrant NF-κB activation in lymphomagenesis[11,14] in a genome-wide fashion. They included focal gain/amplification at the *REL* locus (16.4%) (Fig. 1b) and *TRAF6* locus (5.9%), as well as focal deletions at the *PTEN* locus (5.5%) (Supplementary Figs 1 and 4). However, the most striking finding was the common deletion at 6q23.3 involving a 143-kb segment. It exclusively contained the *A20* gene (also called *TNFAIP3*), a negative regulator of NF-κB activation[3–7,15] (Fig. 1b), which was previously reported as a candidate target of 6q23 deletions in ocular lymphoma[16]. LOH involving the *A20* locus was found in 50 cases, of which 12 showed homozygous deletions as determined by the loss of both alleles in an allele-specific copy number analysis (Fig. 1b, Table 1 and Supplementary Table 4). On the basis of this finding, we searched for possible tumour-specific mutations of *A20* by genomic DNA sequencing of entire coding exons of the gene in the same series of lymphoma samples (Supplementary Fig. 5). Because two out of the three Hodgkin's-lymphoma-derived cell lines had biallelic *A20* deletions/mutations (Supplementary Fig. 6), 24 primary samples from Hodgkin's lymphoma were also analysed for mutations, where

[1]Cancer Genomics Project, Department of [2]Pediatrics, [3]Cell Therapy and Transplantation Medicine, and [4]Hematology and Oncology, Graduate School of Medicine, University of Tokyo, 7-3-1 Hongo, Bunkyo-ku, Tokyo 113-8655, Japan. [5]Core Research for Evolutional Science and Technology, Japan Science and Technology Agency, 4-1-8, Honcho, Kawaguchi-shi, Saitama 332-0012, Japan. [6]Department of Pediatrics, Graduate School of Medicine, Kyoto University, 54 Kawahara-cho, Shogoin, Sakyo-ku, Kyoto 606-8507, Japan. [7]Department of Pathology, Okayama University Graduate School of Medicine, Dentistry and Pharmaceutical Sciences, 2-5-1 Shikata-cho, Kita-ku, Okayama 700-8558, Japan. [8]Division of Pathology, The Cancer Institute of Japanese Foundation for Cancer Research, Japan, 3-10-6 Ariake, Koto-ku, Tokyo 135-8550, Japan. [9]Hematology Division, Hospital, and [10]Early Oncogenesis Research Project, Research Institute, National Cancer Center, 5-1-1 Tsukiji, Chuo-ku, Tokyo 104-0045, Japan. [11]Division of Immunology, Aichi Cancer Center Research Institute, 1-1 Kanokoden, Chikusa-ku, Nagoya 464-8681, Japan. [12]Gunma Children's Medical Center, 779 Shimohakoda, Hokkitsu-machi, Shibukawa 377-8577, Japan. [13]Division of Hematology, Internal Medicine, Showa University Fujigaoka Hospital, 1-30, Fujigaoka, Aoba-ku, Yokohama-shi, Kanagawa 227-8501, Japan. [14]Department of Pathology, Teikyo University School of Medicine, 2-11-1 Kaga, Itabashi-ku, Tokyo 173-8605, Japan.

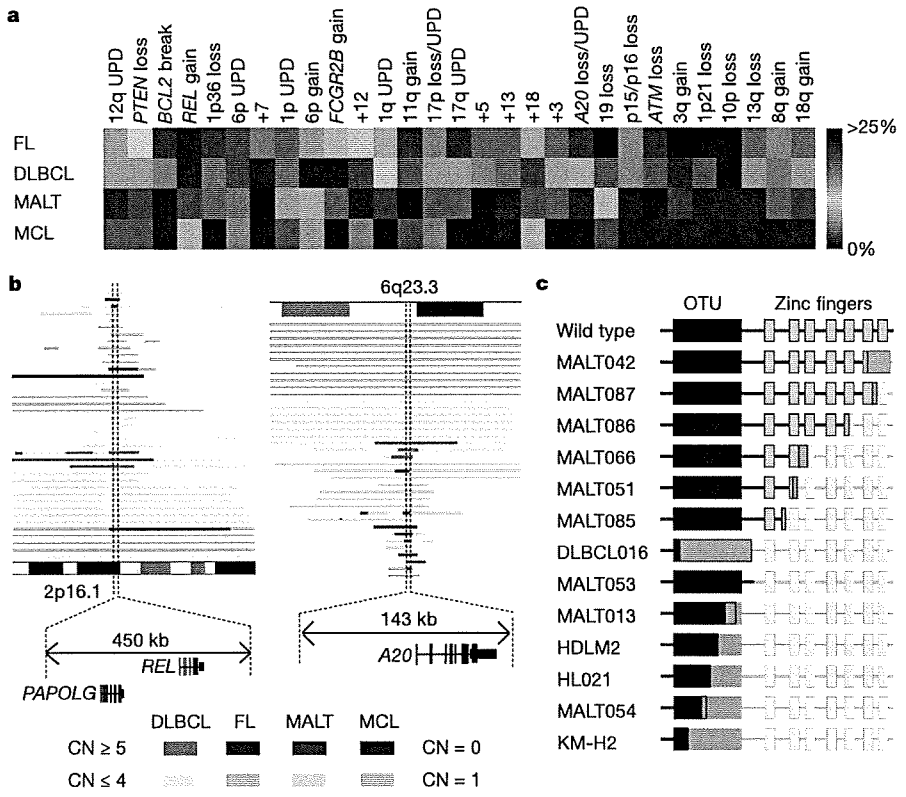

Figure 1 | Genomic signatures of different B-cell lymphomas and common genetic lesions at 2p16-15 and 6q23.3 involving NF-κB pathway genes. **a**, Twenty-nine genetic lesions were found in more than 10% in at least one histology and used for clustering four distinct histology types of B-lineage lymphomas. The frequency of each genetic lesion in each histology type is colour-coded. FL, follicular lymphoma; UPD, uniparental disomy. **b**, Recurrent genetic changes are depicted based on CNAG output of the SNP array analysis of 238 B-lineage lymphoma samples, which include gains at the *REL* locus on 2p16-15 (left panel) and the *A20* locus on 6q23.3 (right panel). Regions showing copy number gain or loss are indicated by horizontal lines. Four histology types are indicated by different colours, where high-grade amplifications and homozygous deletions are shown by darker shades to discriminate from simple gains (copy number ≤4) and losses (copy number = 1) (lighter shades). **c**, Point mutations and small nucleotide insertions and deletions in the *A20* (*TNFAIP3*) gene caused premature truncation of A20 in most cases. Altered amino acids caused by frame shifts are indicated by green bars.

genomic DNA was extracted from 150 microdissected CD30-positive tumour cells (Reed–Sternberg cells) for each sample. *A20* mutations were found in 18 out of 265 lymphoma samples (6.8%) (Table 1), among which 13 mutations, including nonsense mutations (3 cases), frame-shift insertions/deletions (9 cases), and a splicing donor site mutation (1 case) were thought to result in premature termination of translation (Fig. 1c). Four missense mutations and one intronic mutation were identified in five microdissected Hodgkin's lymphoma samples. They were not found in the surrounding normal tissues, and thus, were considered as tumour-specific somatic changes.

In total, biallelic *A20* lesions were found in 31 out of 265 lymphoma samples including 3 Hodgkin's lymphoma cell lines. Quantitative analysis of SNP array data suggested that these *A20* lesions were present in the major tumour fraction within the samples (Supplementary Fig. 7). Inactivation of *A20* was most frequent in MALT lymphoma (18 out of 87) and Hodgkin's lymphoma (7 out of 27), although it was also found in DLBCL (5 out of 64) and follicular lymphoma (1 out of 52) at lower frequencies. In MALT lymphoma, biallelic *A20* lesions were confirmed in 18 out of 24 cases (75.0%) with LOH involving the 6q23.3 segment (Supplementary Fig. 8). Considering the limitation in detecting very small homozygous deletions, *A20* was thought to be the target of 6q23 LOH in MALT lymphoma. On the other hand, the 6q23 LOHs in other histology types tended to be extended into more centromeric regions and less frequently accompanied biallelic *A20* lesions (Supplementary Fig. 8 and Supplementary Table 4), indicating that they might be more heterogeneous with regard to their gene targets. We were unable to analyse Hodgkin's lymphoma samples using SNP arrays owing to insufficient genomic DNA obtained from microdissected samples, and were likely to underestimate the frequency of *A20* inactivation in Hodgkin's lymphoma because we might fail to detect a substantial proportion of cases with homozygous deletions, which explained 50% (12 out of 24) of *A20* inactivation in other histology types. *A20* mutations in Hodgkin's lymphoma were exclusively found in nodular sclerosis classical Hodgkin's lymphoma (5 out of 15) but not in other histology types (0 out of 9), although the possible association requires further confirmation in additional cases.

A20 is a key regulator of NF-κB signalling, negatively modulating NF-κB activation through a wide variety of cell surface receptors and viral proteins, including tumour-necrosis factor (TNF) receptors, toll-like receptors, CD40, as well as Epstein–Barr-virus-associated LMP1 protein[2,5,17,18]. To investigate the role of A20 inactivation in lymphomagenesis, we re-expressed wild-type A20 under a *Tet*-inducible promoter in a lymphoma-derived cell line (KM-H2) that had no functional *A20* alleles (Supplementary Fig. 6), and examined the effect of A20 re-expression on cell proliferation, survival and downstream NF-κB signalling pathways. As shown in Fig. 2a–c and Supplementary Fig. 9, re-expression of wild-type A20 resulted in the suppression of cell proliferation and enhanced apoptosis, and in the concomitant accumulation of IκBβ and IκBε, and downregulation of NF-κB activity. In contrast, re-expression of two lymphoma-derived A20 mutants, $A20^{532Stop}$ or $A20^{750Stop}$, failed to show growth suppression, induction of apoptosis, accumulation of IκBβ and IκBε or downregulation of

Table 1 | Inactivation of A20 in B-lineage lymphomas

Histology	Tissue	Sample	Allele	Uniparental disomy	Exon	Mutation	Biallelic inactivation
DLBCL							5 out of 64 (7.8%)
	Lymph node	DLBCL008	−/−	No	–	–	
	Lymph node	DLBCL016	+/−	No	Ex2	329insA	
	Lymph node	DLBCL022	−/−	No	–	–	
	Lymph node	DLBCL028	−/−	Yes	–	–	
	Lymph node	MCL008*	−/−	Yes	–	–	
Follicular lymphoma							1 out of 52 (1.9%)
	Lymph node	FL024	−/−	No	–	–	
MCL							0 out of 35 (0%)
MALT							18 out of 87 (21.8%)
Stomach							3 out of 23 (13.0%)
	Gastric mucosa	MALT013	+/+	Yes	Ex5	705insG	
	Gastric mucosa	MALT014	+/+	Yes	Ex3	Ex3 donor site>A	
	Gastric mucosa	MALT036	+/−	No	Ex7	delintron6-Ex7†	
Eye							13 out of 43 (30.2%)
	Ocular adnexa	MALT008	−/−	No	–	–	
	Ocular adnexa	MALT017	−/−	No	–	–	
	Ocular adnexa	MALT051	+/−	No	Ex7	1943delTG	
	Ocular adnexa	MALT053	+/+	Yes	Ex6	1016G>A(stop)	
	Ocular adnexa	MALT054	+/−	No	Ex3	502delTC	
	Ocular adnexa	MALT055	−/−	No	–	–	
	Ocular adnexa	MALT066	+/−	No	Ex7	1581insA	
	Ocular adnexa	MALT067	−/−	No	–	–	
	Ocular adnexa	MALT082	−/−	Yes	–	–	
	Ocular adnexa	MALT084	−/−	Yes	–	–	
	Ocular adnexa	MALT085	+/+	Yes	Ex7	1435insG	
	Ocular adnexa	MALT086	+/+	Yes	Ex6	878C>T(stop)	
	Ocular adnexa	MALT087	+/+	Yes	Ex9	2304delGG	
Lung							2 out of 12 (16.7%)
	Lung	MALT042	−/−	No	–	–	
	Lung	MALT047	+/+	Yes	Ex9	2281insT	
Other‡							0 out of 9 (0%)
Hodgkin's lymphoma							7 out of 27 (26.0%)
NSHL	Lymph node	HL10	ND	ND	Ex7	1777G>A(V571I)	
NSHL	Lymph node	HL12	ND	ND	Ex7	1156A>G(R364G)	
NSHL	Lymph node	HL21	ND	ND	Ex4	569G>A(stop)	
NSHL	Lymph node	HL24	ND	ND	Ex3	1487C>A(T474N)	
NSHL	Lymph node	HL23	ND	ND	–	Intron 3§	
	Cell line	KM-H2	−/−	No	–		
	Cell line	HDLM2	+/−	No	Ex4	616ins29bp‖	
Total							31 out of 265 (11.7%)

DLBCL, diffuse large B-cell lymphoma; MALT, MALT lymphoma; MCL, mantle cell lymphoma; ND, not determined because SNP array analysis was not performed; NSHL, nodular sclerosis classical Hodgkin's lymphoma.
* Diagnosis was changed based on the genomic data, which was confirmed by re-examination of pathology.
† Deletion including the boundary of intron 6 and exon 7 (see also Supplementary Fig. 5b).
‡ Including 1 parotid gland, 1 salivary gland, 2 colon and 5 thyroid cases.
§ Insertion of CTC at −19 bases from the beginning of exon 3.
‖ Insertion of TGGCTTCCACAGACACACCCATGGCCCGA.

NF-κB activity (Fig. 2a–c), indicating that these were actually loss-of-function mutations. To investigate the role of A20 inactivation in lymphomagenesis *in vivo*, *A20*- and mock-transduced KM-H2 cells were transplanted in NOD/SCID/γ_c^{null} (NOG) mice[19], and their tumour formation status was examined for 5 weeks with or without induction of wild-type A20 by tetracycline administration. As shown in Fig. 2d, mock-transduced cells developed tumours at the injected sites, whereas the *Tet*-inducible *A20*-transduced cells generated tumours only in the absence of A20 induction (Supplementary Table 5), further supporting the tumour suppressor role of A20 in lymphoma development.

Given the mode of negative regulation of NF-κB signalling, we next investigated the origins of NF-κB activity that was deregulated by A20 loss in KM-H2 cells. The conditioned medium prepared from a 48-h serum-free KM-H2 culture had increased NF-κB upregulatory activity compared with fresh serum-free medium, which was inhibited by re-expression of A20 (Fig. 3a). KM-H2 cells secreted two known ligands for TNF receptor—TNF-α and lymphotoxin-α (Supplementary Fig. 10)[20]—and adding neutralizing antibodies against these cytokines into cultures significantly suppressed their cell growth and NF-κB activity without affecting the levels of their overall suppression after A20 induction (Fig. 3b, d). In addition, recombinant TNF-α and/or lymphotoxin-α added to fresh serum-free medium promoted cell growth and NF-κB activation in KM-H2 culture, which were again suppressed by re-expression of A20 (Fig. 3c, e). Although our data in Fig. 3 also show the presence of factors other than TNF-α and lymphotoxin-α in the KM-H2-conditioned medium—as well as some intrinsic pathways in the cell (Fig. 3a)—that were responsible for the A20-dependent NF-κB activation, these results indicate that both cell growth and NF-κB activity that were upregulated by A20 inactivation depend at least partly on the upstream stimuli that evoked the NF-κB-activating signals.

Aberrant activation of the NF-κB pathway is a hallmark of several subtypes of B-lineage lymphomas, including Hodgkin's lymphoma, MALT lymphoma, and a subset of DLBCL, as well as other lymphoid neoplasms[11,14], where a number of genetic alterations of NF-κB signalling pathway genes[21–25], as well as some viral proteins[26,27], have been implicated in the aberrant activation of the NF-κB pathway[14]. Thus, frequent inactivation of A20 in Hodgkin's lymphoma and MALT and other lymphomas provides a novel insight into the molecular pathogenesis of these subtypes of B-lineage lymphomas through deregulated NF-κB activation. Because A20 provides a

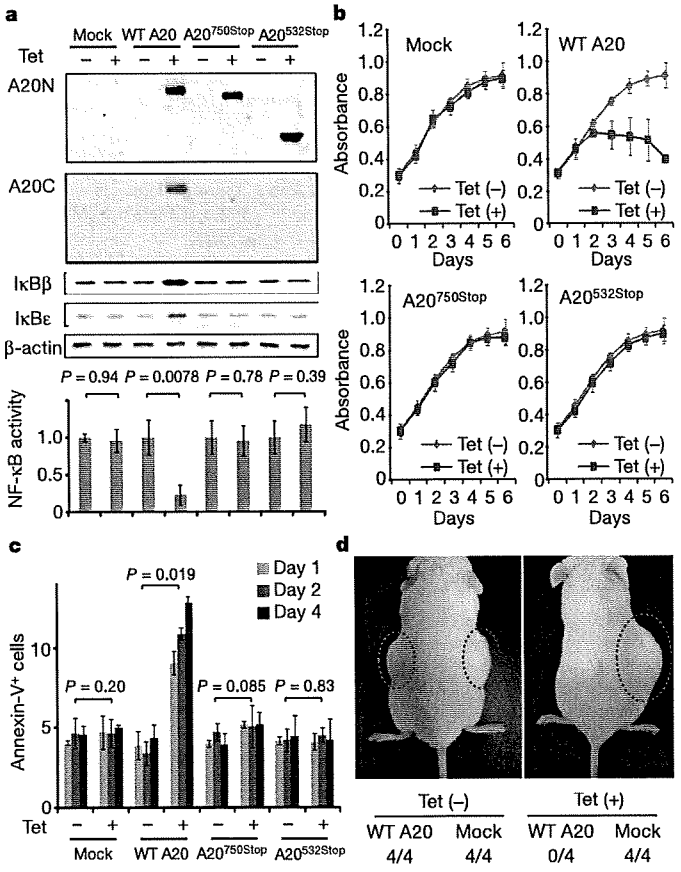

Figure 2 | Effects of wild-type and mutant A20 re-expressed in a lymphoma cell line that lacks the normal *A20* gene. a, Western blot analyses of wild-type (WT) and mutant ($A20^{532Stop}$ and $A20^{750Stop}$) A20, as well as IκBβ and IκBε, in KM-H2 cells, in the presence or absence of tetracycline treatment (top panels). A20N and A20C are polyclonal antisera raised against N-terminal and C-terminal A20 peptides, respectively. β-actin blots are provided as a control. NF-κB activities are expressed as mean absorbance ± s.d. ($n = 6$) in luciferase assays (bottom panel). **b,** Proliferation of KM-H2 cells stably transduced with plasmids for mock and *Tet*-inducible wild-type A20, $A20^{532Stop}$ and $A20^{750Stop}$ was measured using a cell counting kit in the presence (red lines) or absence (blue lines) of tetracycline. Mean absorbance ± s.d. ($n = 5$) is plotted. **c,** The fractions of Annexin-V-positive KM-H2 cells transduced with various *Tet*-inducible A20 constructs were measured by flow cytometry after tetracycline treatment and the mean values (±s.d., $n = 3$) are plotted. **d,** *In vivo* tumorigenicity was assayed by inoculating 7×10^6 KM-H2 cells transduced with mock or *Tet*-inducible wild-type A20 in NOG mice, with (right panel) or without (left panel) tetracycline administration.

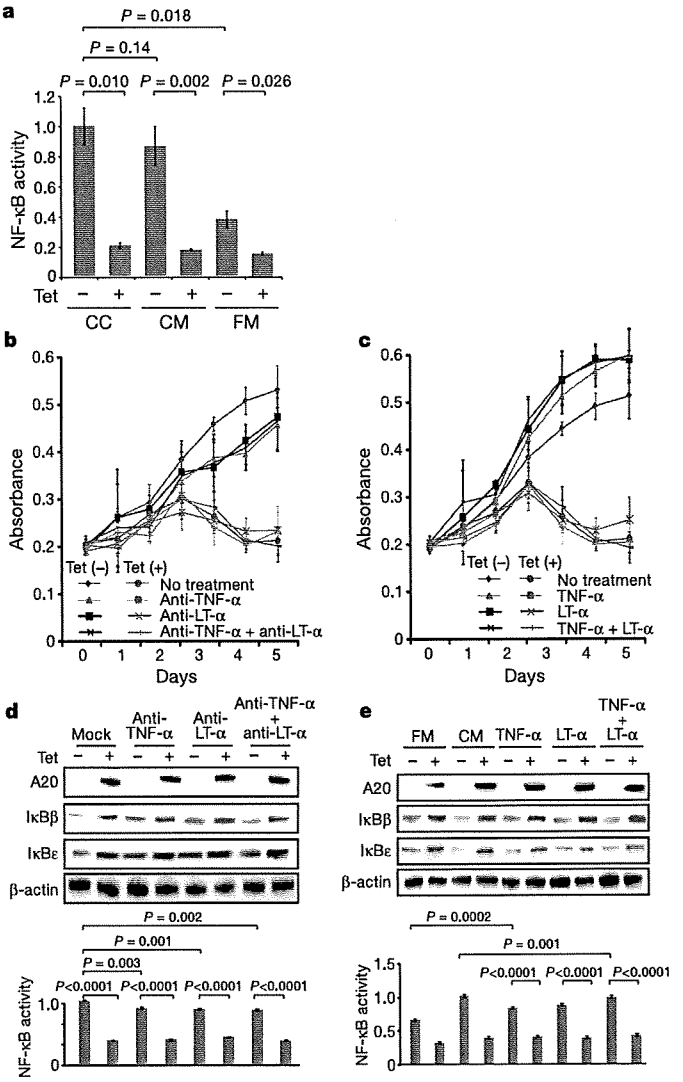

Figure 3 | Tumour suppressor role of A20 under external stimuli. a, NF-κB activity in KM-H2 cells was measured 30 min after cells were inoculated into fresh medium (FM) or KM-H2-conditioned medium (CM) obtained from the 48-h culture of KM-H2, and was compared with the activity after 48 h continuous culture of KM-H2 (CC). A20 was induced 12 h before inoculation in Tet (+) groups. **b, c,** Effects of neutralizing antibodies against TNF-α and lymphotoxin-α (LTα) (**b**) and of recombinant TNF-α and LT-α added to the culture (**c**) on cell growth were evaluated in the presence (Tet (+)) or absence (Tet (−)) of A20 induction. Cell numbers were measured using a cell counting kit and are plotted as their mean absorbance ± s.d. ($n = 6$). **d, e,** Effects of the neutralizing antibodies (**d**) and the recombinant cytokines added to the culture (**e**) on NF-κB activities and the levels of IκBβ and IκBε after 48 h culture with (Tet (+)) or without (Tet (−)) tetracycline treatment. NF-κB activities are expressed as mean absorbance ± s.d. ($n = 6$) in luciferase assays.

negative feedback mechanism in the regulation of NF-κB signalling pathways upon a variety of stimuli, aberrant activation of NF-κB will be a logical consequence of A20 inactivation. However, there is also the possibility that the aberrant NF-κB activity of A20-inactivated lymphoma cells is derived from upstream stimuli, which may be from the cellular environment. In this context, it is intriguing that MALT lymphoma usually arises at the site of chronic inflammation caused by infection or autoimmune disorders and may show spontaneous regression after eradication of infectious organisms[28]; furthermore, Hodgkin's lymphoma frequently shows deregulated cytokine production from Reed–Sternberg cells and/or surrounding reactive cells[29]. Detailed characterization of the NF-κB pathway regulated by A20 in both normal and neoplastic B lymphocytes will promote our understanding of the precise roles of A20 inactivation in the pathogenesis of these lymphoma types. Our finding underscores the importance of genome-wide approaches in the identification of genetic targets in human cancers.

METHODS SUMMARY

Genomic DNA from 238 patients with non-Hodgkin's lymphoma and three Hodgkin's-lymphoma-derived cell lines was analysed using GeneChip SNP genotyping microarrays (Affymetrix). This study was approved by the ethics boards of the University of Tokyo, National Cancer Institute Hospital, Okayama University, and the Cancer Institute of the Japanese Foundation of Cancer Research. After appropriate normalization of mean array intensities, signal ratios between tumours and anonymous normal references were calculated in an allele-specific manner, and allele-specific copy numbers were inferred from the observed signal ratios based on the hidden Markov model using CNAG/AsCNAR software (http://www.genome.umin.jp). *A20* mutations were examined by directly sequencing genomic DNA using a set of primers (Supplementary Table 6). Full-length cDNAs of wild-type and mutant *A20* were introduced into a

lentivirus vector, pLenti4/TO/V5-DEST (Invitrogen), with a *Tet*-inducible promoter. Viral stocks were prepared by transfecting the vector plasmids into 293FT cells (Invitrogen) using the calcium phosphate method and then infected to the KM-H2 cell line. Proliferation of KM-H2 cells was measured using a Cell Counting Kit (Dojindo). Western blot analyses and luciferase assays were performed as previously described. NF-κB activity was measured by luciferase assays in KM-H2 cells stably transduced with a reporter plasmid having an NF-κB response element, pGL4.32 (Promega). Apoptosis of KM-H2 upon A20 induction was evaluated by counting Annexin-V-positive cells by flow cytometry. For *in vivo* tumorigenicity assays, 7×10^6 KM-H2 cells were transduced with the *Tet*-inducible *A20* gene and those with a mock vector were inoculated on the contralateral sides in eight NOG mice[19] and examined for their tumour formation with ($n = 4$) or without ($n = 4$) tetracycline administration. Full copy number data of the 238 lymphoma samples will be accessible from the Gene Expression Omnibus (GEO, http://ncbi.nlm.nih.gov/geo/) with the accession number GSE12906.

Full Methods and any associated references are available in the online version of the paper at www.nature.com/nature.

Received 17 September 2008; accepted 3 March 2009.
Published online 3 May 2009.

1. Dixit, V. M. *et al.* Tumor necrosis factor-α induction of novel gene products in human endothelial cells including a macrophage-specific chemotaxin. *J. Biol. Chem.* **265**, 2973–2978 (1990).
2. Song, H. Y., Rothe, M. & Goeddel, D. V. The tumor necrosis factor-inducible zinc finger protein A20 interacts with TRAF1/TRAF2 and inhibits NF-κB activation. *Proc. Natl Acad. Sci. USA* **93**, 6721–6725 (1996).
3. Lee, E. G. *et al.* Failure to regulate TNF-induced NF-κB and cell death responses in A20-deficient mice. *Science* **289**, 2350–2354 (2000).
4. Boone, D. L. *et al.* The ubiquitin-modifying enzyme A20 is required for termination of Toll-like receptor responses. *Nature Immunol.* **5**, 1052–1060 (2004).
5. Wang, Y. Y., Li, L., Han, K. J., Zhai, Z. & Shu, H. B. A20 is a potent inhibitor of TLR3- and Sendai virus-induced activation of NF-κB and ISRE and IFN-β promoter. *FEBS Lett.* **576**, 86–90 (2004).
6. Wertz, I. E. *et al.* De-ubiquitination and ubiquitin ligase domains of A20 downregulate NF-κB signalling. *Nature* **430**, 694–699 (2004).
7. Heyninck, K. & Beyaert, R. A20 inhibits NF-κB activation by dual ubiquitin-editing functions. *Trends Biochem. Sci.* **30**, 1–4 (2005).
8. Graham, R. R. *et al.* Genetic variants near *TNFAIP3* on 6q23 are associated with systemic lupus erythematosus. *Nature Genet.* **40**, 1059–1061 (2008).
9. Musone, S. L. *et al.* Multiple polymorphisms in the *TNFAIP3* region are independently associated with systemic lupus erythematosus. *Nature Genet.* **40**, 1062–1064 (2008).
10. Jaffe, E. S., Harris, N. L., Stein, H. & Vardiman, J. W. *World Health Organization Classification of Tumours. Pathology and Genetics of Tumours of Hematopoietic and Lymphoid Tissues* (IARC Press, 2001).
11. Klein, U. & Dalla-Favera, R. Germinal centres: role in B-cell physiology and malignancy. *Nature Rev. Immunol.* **8**, 22–33 (2008).
12. Nannya, Y. *et al.* A robust algorithm for copy number detection using high-density oligonucleotide single nucleotide polymorphism genotyping arrays. *Cancer Res.* **65**, 6071–6079 (2005).
13. Yamamoto, G. *et al.* Highly sensitive method for genomewide detection of allelic composition in nonpaired, primary tumor specimens by use of affymetrix single-nucleotide-polymorphism genotyping microarrays. *Am. J. Hum. Genet.* **81**, 114–126 (2007).
14. Jost, P. J. & Ruland, J. Aberrant NF-κB signaling in lymphoma: mechanisms, consequences, and therapeutic implications. *Blood* **109**, 2700–2707 (2007).
15. Durkop, H., Hirsch, B., Hahn, C., Foss, H. D. & Stein, H. Differential expression and function of A20 and TRAF1 in Hodgkin lymphoma and anaplastic large cell lymphoma and their induction by CD30 stimulation. *J. Pathol.* **200**, 229–239 (2003).
16. Honma, K. *et al. TNFAIP3* is the target gene of chromosome band 6q23.3-q24.1 loss in ocular adnexal marginal zone B cell lymphoma. *Genes Chromosom. Cancer* **47**, 1–7 (2008).
17. Sarma, V. *et al.* Activation of the B-cell surface receptor CD40 induces A20, a novel zinc finger protein that inhibits apoptosis. *J. Biol. Chem.* **270**, 12343–12346 (1995).
18. Fries, K. L., Miller, W. E. & Raab-Traub, N. The A20 protein interacts with the Epstein-Barr virus latent membrane protein 1 (LMP1) and alters the LMP1/TRAF1/TRADD complex. *Virology* **264**, 159–166 (1999).
19. Hiramatsu, H. *et al.* Complete reconstitution of human lymphocytes from cord blood $CD34^+$ cells using the NOD/SCID/γ^{null} mice model. *Blood* **102**, 873–880 (2003).
20. Hsu, P. L. & Hsu, S. M. Production of tumor necrosis factor-α and lymphotoxin by cells of Hodgkin's neoplastic cell lines HDLM-1 and KM-H2. *Am. J. Pathol.* **135**, 735–745 (1989).
21. Dierlamm, J. *et al.* The apoptosis inhibitor gene *API2* and a novel 18q gene, *MLT*, are recurrently rearranged in the t(11;18)(q21;q21) associated with mucosa-associated lymphoid tissue lymphomas. *Blood* **93**, 3601–3609 (1999).
22. Willis, T. G. *et al.* Bcl10 is involved in t(1;14)(p22;q32) of MALT B cell lymphoma and mutated in multiple tumor types. *Cell* **96**, 35–45 (1999).
23. Joos, S. *et al.* Classical Hodgkin lymphoma is characterized by recurrent copy number gains of the short arm of chromosome 2. *Blood* **99**, 1381–1387 (2002).
24. Martin-Subero, J. I. *et al.* Recurrent involvement of the *REL* and *BCL11A* loci in classical Hodgkin lymphoma. *Blood* **99**, 1474–1477 (2002).
25. Lenz, G. *et al.* Oncogenic *CARD11* mutations in human diffuse large B cell lymphoma. *Science* **319**, 1676–1679 (2008).
26. Deacon, E. M. *et al.* Epstein-Barr virus and Hodgkin's disease: transcriptional analysis of virus latency in the malignant cells. *J. Exp. Med.* **177**, 339–349 (1993).
27. Yin, M. J. *et al.* HTLV-I Tax protein binds to MEKK1 to stimulate IκB kinase activity and NF-κB activation. *Cell* **93**, 875–884 (1998).
28. Isaacson, P. G. & Du, M. Q. MALT lymphoma: from morphology to molecules. *Nature Rev. Cancer* **4**, 644–653 (2004).
29. Skinnider, B. F. & Mak, T. W. The role of cytokines in classical Hodgkin lymphoma. *Blood* **99**, 4283–4297 (2002).

Supplementary Information is linked to the online version of the paper at www.nature.com/nature.

Acknowledgements This work was supported by the Core Research for Evolutional Science and Technology, Japan Science and Technology Agency, by the 21st century centre of excellence program 'Study on diseases caused by environment/genome interactions', and by Grant-in-Aids from the Ministry of Education, Culture, Sports, Science and Technology of Japan and from the Ministry of Health, Labor and Welfare of Japan for the 3rd-term Comprehensive 10-year Strategy for Cancer Control. We also thank Y. Ogino, E. Matsui and M. Matsumura for their technical assistance.

Author Contributions M.Ka., K.N. and M.S. performed microarray experiments and subsequent data analyses. M.Ka., Y.C., K.Ta., J.T., J.N., M.I., A.T. and Y.K. performed mutation analysis of *A20*. M.Ka., S.Mu., M.S., Y.C. and Y.Ak. conducted functional assays of mutant A20. Y.S., K.Ta., Y.As., H.M., M.Ku., S.Mo., S.C., Y.K., K.To. and Y.I. prepared tumour specimens. I.K., K.O., A.N., H.N. and T.N. conducted *in vivo* tumorigenicity experiments in NOG/SCID mice. T.I., Y.H., T.Y., Y.K. and S.O. designed overall studies, and S.O. wrote the manuscript. All authors discussed the results and commented on the manuscript.

Author Information The copy number data as well as the raw microarray data will be accessible from the GEO (http://ncbi.nlm.nih.gov/geo/) with the accession number GSE12906. Reprints and permissions information is available at www.nature.com/reprints. Correspondence and requests for materials should be addressed to S.O. (sogawa-tky@umin.ac.jp) or Y.K. (ykkobaya@ncc.go.jp).

METHODS

Specimens. Primary tumour specimens were obtained from patients who were diagnosed with DLBCL, follicular lymphoma, MCL, MALT lymphoma, or classical Hodgkin's lymphoma. In total, 238 primary lymphoma specimens listed in Supplementary Table 1 were subjected to SNP array analysis. Three Hodgkin's-lymphoma-derived cell lines (KM-H2, HDLM2, L540) were obtained from Hayashibara Biochemical Laboratories, Inc., Fujisaki Cell Center and were also analysed by SNP array analysis.

Microarray analysis. High-molecular-mass DNA was isolated from tumour specimens and subjected to SNP array analysis using GeneChip Mapping 50K and/or 250K arrays (Affymetrix). The scanned array images were processed with Gene Chip Operation software (GCOS), followed by SNP calls using GTYPE. Genome-wide copy number measurements and LOH detection were performed using CNAG/AsCNAR software[12,13].

Mutation analysis. Mutations in the *A20* gene were examined in 265 samples of B-lineage lymphoma, including 62 DLBCLs, 52 follicular lymphomas, 87 MALTs, 37 MCLs and 3 Hodgkin's-lymphoma-derived cell lines and 24 primary Hodgkin's lymphoma samples, by direct sequencing using an ABI PRISM 3130xl Genetic Analyser (Applied Biosystems). To analyse primary Hodgkin's lymphoma samples in which CD30-positive tumour cells (Reed–Sternberg cells) account for only a fraction of the specimen, 150 Reed–Sternberg cells were collected for each 10 μm slice of a formalin-fixed block immunostained for CD30 by laser-capture microdissection (ASLMD6000, Leica), followed by genomic DNA extraction using QIAamp DNA Micro kit (Qiagen). The primer sets used in this study are listed in Supplementary Table 6.

Functional analysis of wild-type and mutant A20. Full-length cDNA for wild-type *A20* was isolated from total RNA extracted from an acute myeloid leukaemia-derived cell line, CTS, and subcloned into a lentivirus vector (pLenti4/TO/V5-DEST, Invitrogen). cDNAs for mutant A20 were generated by PCR amplification using mutagenic primers (Supplementary Table 6), and introduced into the same lentivirus vector. Forty-eight hours after transfection of each plasmid into 293FT cells using the calcium phosphate method, lentivirus stocks were obtained from ultrafiltration using Amicon Ultra (Millipore), and used to infect KM-H2 cells to generate stable transfectants of mock, wild-type and mutant A20. Each KM-H2 derivative cell line was further transduced stably with a reporter plasmid (pGL4.32, Promega) containing a luciferase gene under an NF-κB-responsive element by electroporation using Nucleofector reagents (Amaxa).

Assays for cell proliferation and NF-κB activity. Proliferation of the KM-H2 derivative cell lines was assayed in triplicate using a Cell Counting Kit (Dojindo). The mean absorption of five independent assays was plotted with s.d. for each derivative line. Two independent KM-H2-derived cell lines were used for each experiment. The NF-κB activity in KM-H2 derivatives for A20 mutants was evaluated by luciferase assays using a PiccaGene Luciferase Assay Kit (TOYO B-Net Co.). Each assay was performed in triplicate and the mean absorption of five independent experiments was plotted with s.d.

Western blot analyses. Polyclonal anti-sera against N-terminal (anti-A20N) and C-terminal (anti-A20C) A20 peptides were generated by immunizing rabbits with these peptides (LSNMRKAVKIRERTPEDIC for anti-A20N and CFQFKQMYG for anti-A20C, respectively). Total cell lysates from KM-H2 cells were separated on 7.5% polyacrylamide gel and subjected to western blot analysis using antibodies to A20 (anti-A20N and anti-A20C), IκBα (sc-847), IκBβ (sc-945), IκBγ (sc-7155) and actin (sc-8432) (Santa Cruz Biotechnology).

Functional analyses of wild-type and mutant A20. Each KM-H2 derivative cell line stably transduced with various *Tet*-inducible A20 constructs was cultured in serum-free medium in the presence or absence of A20 induction using 1 μg ml^{-1} of tetracycline, and cell number was counted every day. 1×10^6 cells of each KM-H2 derivative cell line were analysed for their intracellular levels of IκBβ and IκBε and for NF-κB activities by western blot analyses and luciferase assays, respectively, 12 h after the beginning of cell culture. Effects of human recombinant TNF-α and lymphotoxin-α (210-TA and 211-TB, respectively, R&D Systems) on the NF-κB pathway and cell proliferation were evaluated by adding both cytokines into 10 ml of serum-free cell culture at a concentration of 200 pg ml^{-1}. For cell proliferation assays, culture medium was half replaced every 12 h to minimize the side-effects of autocrine cytokines. Intracellular levels of IκBβ, IκBε and NF-κB were examined 12 h after the beginning of the cell culture. To evaluate the effect of neutralizing TNF-α and lymphotoxin-α, 1×10^6 of KM-H2 cells transduced with both *Tet*-inducible A20 and the NF-κB-luciferase reporter were pre-cultured in serum-free media for 36 h, and thereafter neutralizing antibodies against TNF-α (MAB210, R&D Systems) and/or lymphotoxin-α (AF-211-NA, R&D Systems) were added to the media at a concentration of 200 pg ml^{-1}. After the extended culture during 12 h with or without 1 μg ml^{-1} tetracycline, the intracellular levels of IκBβ and IκBε and NF-κB activities were examined by western blot analysis and luciferase assays, respectively. To examine the effects of A20 re-expression on apoptosis, 1×10^6 KM-H2 cells were cultured for 4 days in 10 ml medium with or without *Tet* induction. After staining with phycoerythrin-conjugated anti-Annexin-V (ID556422, Becton Dickinson), Annexin-V-positive cells were counted by flow cytometry at the indicated times.

***In vivo* tumorigenicity assays.** KM-H2 cells transduced with a mock or *Tet*-inducible wild-type *A20* gene were inoculated into NOG mice and their tumorigenicity was examined for 5 weeks with or without tetracycline administration. Injections of 7×10^6 cells of each KM-H2 cell line were administered to two opposite sites in four mice. Tetracycline was administered in drinking water at a concentration of 200 μg ml^{-1}.

ELISA. Concentrations of TNF-α, lymphotoxin-α, IL-1, IL-2, IL-4, IL-6, IL-12, IL-18 and TGF-β in the culture medium were measured after 48 h using ELISA. For those cytokines detectable after 48-h culture (TNFα, LTα, and IL-6), their time course was examined further using the Quantikine ELISA kit (R&D Systems).

Statistical analysis. Significance of the difference in NF-κB activity between two given groups was evaluated using a paired *t*-test, in which the data from each independent luciferase assay were paired to calculate test statistics. To evaluate the effect of A20 re-expression in KM-H2 cells on apoptosis, the difference in the fractions of Annexin-V-positive cells between Tet (+) and Tet (−) groups was also tested by a paired *t*-test for assays, in which the data from the assays performed on the same day were paired.